2007

IR-UWB for multiple-access with differential-detection receiver

Walid M. Mahmoud

University of Windsor

IR-UWB FOR MULTIPLE-ACCESS WITH DIFFERENTIAL-DETECTION RECEIVER

BY

Walid M. Mahmoud

A Thesis
Submitted to the Faculty of Graduate Studies
through Electrical Engineering
in Partial Fulfillment of the Requirements for
the Degree of Master of Applied Science at the
University of Windsor

Windsor, Ontario, Canada

2007

Your file Votre référence
ISBN: 978-0-494-34932-8
Our file Notre référence
ISBN: 978-0-494-34932-8

ABSTRACT

IR-UWB FOR MULTIPLE-ACCESS WITH DIFFERENTIAL-DETECTION RECEIVER

BY

WALID M. MAHMOUD

Impulse-Radio Ultra-Wideband (IR-UWB) emerged as a new wireless technology because of its unique characteristics. Such characteristics are the ability to support rich-multimedia applications over short-ranges, the ability to share the available spectrum among multi-users, and the ability to design less complex transceivers for wireless communication systems functioning based on this technology. In this thesis a novel noncoherent IR-UWB receiver designed to support multiple-access is proposed. The transmitter of the proposed system employs the noncoherent bit-level differential phase-shift keying modulation combined with direct-sequence code division multiple-access. The system is investigated under the effect of the additive white Gaussian noise with multiple-access channel. The receiver implements bit-level differential-detection to recover information bits. Closed-form expression for the average probability of error in the proposed receiver while considering the channel effects is analytically derived. This receiver is compared against another existing coherent receiver in terms of bit error rate performance to confirm its practicality. The proposed receiver is characterized by its simple design requirements and its multiple-access efficiency.

DEDICATION

This thesis is dedicated to my lovely parents, Mustafa and Yusra, and my brother Mufeed who have supported me all the way since the beginning of my studies. Also, this thesis is dedicated to my wife Layla and our children who have been a great source of motivation and inspiration.

ACKNOWLEDGMENTS

At the very beginning of my M.A.Sc journey two years ago, I was wondering about the possibility of success on my own without the help and support of other people. Indeed, many individuals have played vital roles during my journey and have assisted me when I was in need. First of all, I would like to thanks my supervisors, Dr. Kemal and Dr. Esam for their patience, continuous support and encouragement. In addition to my supervisors, a special thanks for the committee members who share their ideas, suggestions on my work and their comments on this thesis. I want to give my special thanks to my brother, Dr. Mufeed, for his continual support and motivation. He has provided me with guidance and a sense of direction through all phases of my research work. My deepest appreciation and thanks for my lovely parents, who gave me a great education and taught me all the positive attitudes. Your patience, support and encouragement will always be engraved in my heart. Finally, but not the last, I would like to express my deepest gratitude and appreciation to my wife Layla, my son Mustafa and my daughter Yusra, for their patience, support and motivation; without them, I could not have successfully completed this thesis. To all of them, I express my sincere gratitude.

CONTENTS

LIST OF TABLES

LIST OF FIGURES

CHAPTER 1

INTRODUCTION

1.1 Motivation

The ever increasing demand to support rich-multimedia applications over short-range connectivity, plays an important role for devising new wireless technologies for the forth generation (4G) wireless communication systems. Such systems are the 4G wireless personal area network (WPAN) communication systems. These systems are required to be simple in their hardware design for low power consumption concerns. They are also required to have a wide bandwidth necessary to support multimedia applications, and to support multiple-access (MA) environments because multi-users are expected to share the available spectrum.

Ultra-Wideband (UWB) is a new wireless technology that is expected to satisfy all the requirements of the 4G WPAN communication systems because of its attractive features. The Federal Communications Commission (FCC) in USA has approved UWB technology for commercial use in February 2002 [1]. UWB communication systems depending on their propagated radio are intended to follow either Impulse-Radio Ultra-wideband (IR-UWB) or Multi-Carrier Ultra-wideband (MC-UWB) technologies [2].

As claimed by the proponents of IR-UWB technology, UWB communication systems designed based on this technology have attractive characteristics, such as simple hardware design due to baseband transmission capability. In addition, the transmission radio of these systems consist of a stream of subsequent pulses, each is an extremely short-duration pulse in time, in the nanosecond order or even less, that has a broad instantaneous bandwidth with very low power spectral density. Furthermore, the transmission power of these systems is very low, which entitles IR-UWB communication systems to be good candidates for the short-range applications. Since the aforementioned characteristics are in match with the requirements of the 4G WPAN communication systems, UWB technology has been accepted as an alternative physical layer standard for these systems [3]. Although IR-UWB communication systems are expected to work at baseband level, practical systems still need to utilize carrier signal during their communications [4, 5].

Possible modulation schemes that can be used with IR-UWB are binary phase-shift keying (BPSK), differential phase-shift keying (DPSK), pulse position modulation (PPM), pulse amplitude modulation (PAM) and on-off keying (OOK) [6]. Depending on the employed modulation scheme at the transmitter device, the receivers in IR-UWB communication systems are classified either as coherent or noncoherent receivers [7, 8]. Noncoherent receivers are simple in their design when compared to coherent receivers, but their bit error rate (BER) performance is less than that of coherent receivers by values up to 3dBs [9]. Both coherent and noncoherent IR-UWB communication systems are already addressed and studied in literature. The proliferation of IR-UWB communication systems in wireless market is evident from the current amount of active research on these systems. Academic researchers and interested groups of industry leaders are actively proposing new ideas for wireless communication systems functioning based on IR-UWB technology [10, 11, 12, 13].

The previously proposed IR-UWB communication systems in [14, 15] are examples on coherent systems. In those systems, coherent modulation like BPSK is employed at the transmitter which requires coherent demodulation at the receiver. The binary data stream in [15], which represents the binary information bits to be conveyed for its final destination, after experiencing BPSK modulation, it modulates the phase of the carrier signal before transmission at the output of the transmitter. Therefore, a carrier recovery circuit is required to extract the carrier-phase from the received signal in the demodulation process in the receiver [16].

For simplicity reasons and if phase synchronization is not the main research topic, in theory the authors suffice by assuming that the receiver has achieved phase synchronization with the received signal without including the carrier recovery circuit, as reported in [14, 15]. In practice, any coherent communication system that employs any form of coherent modulation should has the carrier recovery circuit as the primary component for the demodulator in the receiving device. Figure 1.1 depicts the previously proposed coherent system in [15] for IR-UWB communication systems, which is capable of supporting MA environments.

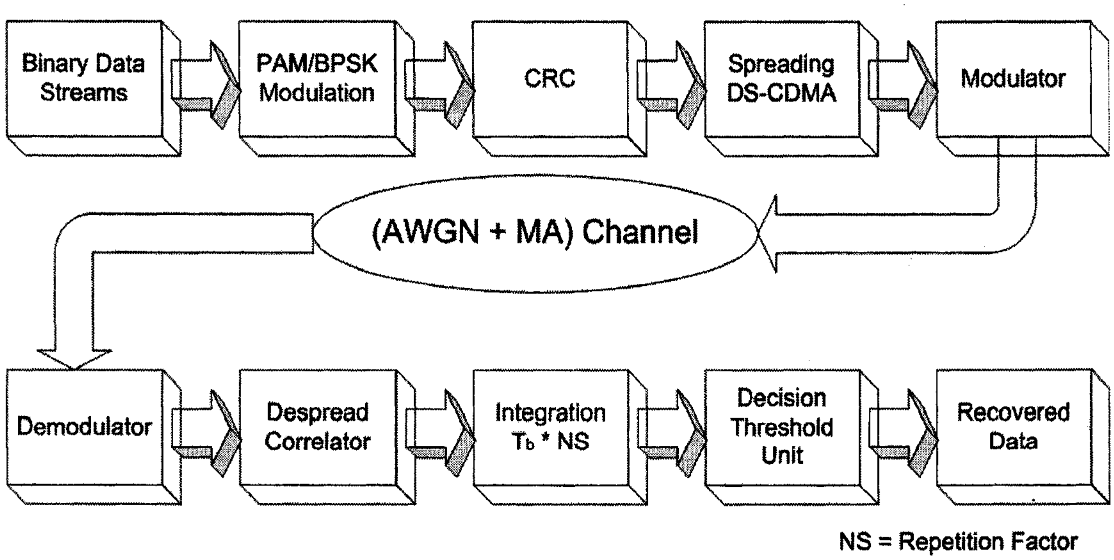

Figure 1.1: DS-BPSK System

When multi-path fading is the dominant channel effect on the transmitted signals, the coherent system in [15] requires full channel estimation, which is necessary to capture and track the amplitude, delay and phase of the scattered components for coherent demodulation at the receiver [17]. The carrier recovery circuit and the full channel estimation requirements add design complexity for coherent IR-UWB receivers.

Noncoherent IR-UWB communication systems that employ bit-level DPSK modulation combined with direct-sequence code division multiple-access (DS-CDMA) for MA support, which implements bit-level differential-detection at receiver side are not examined widely in communications literature. The authors in [18] proposed two innovative bit-level differential-detection receivers for IR-UWB communication systems that employ bit-level DPSK modulation at the transmitter device. These receivers have relaxed the requirement for the carrier recovery circuit because of differential-detection, which permits the use of the previous bit-long signaling interval for demodulation and to recover the originally transmitted information bits. Although their communication systems have been represented mathematically to implement DPSK modulation combined with time hopping code division multiple-access (TH-CDMA) for MA support, the authors did not consider MA capability and focused only on analyzing the systems for the single active-user case. The main focus of [18] was to use limiters at different branches of the receiver to avoid the use of the complex analog multipliers. The authors have acknowledged the ability of these receivers to relax the channel estimation requirement.

In [19] the authors have proposed pulse-level differential-detection receiver for IR-UWB communication systems that employ pulse-level DPSK modulation at the transmitter. The receiver has relaxed the requirement for the carrier recovery circuit because of differential-detection, which permits the use of the previous pulse-long signaling interval for demodulation and recovering the originally transmitted information bits. The authors have focused only on analyzing the receiver for the single active-user case. In [19], the research work did not consider any channel accessing scheme for MA support, therefore the receiver is not capable of supporting MA environments. The receiver was investigated under the effect of multi-path fading channel and was compared against another receiver, namely the rake receiver, to verify its ability to capture the energy of the scattered multi-path components. The authors have acknowledged that the receiver is capable of relaxing the channel estimation requirement.

The attractive features of differential-detection (noncoherent) IR-UWB receivers, such as their simple design requirements, as a result of their ability to relax the carrier recovery circuit and the full channel estimation, are the main reasons for proposing our novel differential-detection receiver for IR-UWB communication systems.

1.2 Research Goals

In this thesis, a novel noncoherent receiver that supports multiple-access (MA) is proposed for IR-UWB communication systems. Because the transmitter of the proposed system employs bit-level differential phase-shift keying (DPSK) modulation, the proposed noncoherent receiver works based on bit-level differential-detection scheme. The MA environment in the proposed system is provided by implementing direct-sequence code division multiple-access (DS-CDMA) protocol, which is widely used in narrowband and wideband communication systems, however, in this work it is used in the context of UWB technology. Therefore, the correlator is an essential component in the receiver and is necessary to despread the received signal. Because of using DS-CDMA for MA support combined with DPSK modulation, the proposed system is referred to as DS-DPSK.

The proposed receiver in DS-DPSK system is compared in terms of BER performance with the performance of the coherent receiver in DS-BPSK system, which is shown in Figure 1.1. Because DS-BPSK system employs BPSK modulation, its receiver device has excellent BER performance. The optimal BER performance of DS-BPSK receiver, in addition to its unique properties those match the properties of the proposed DS-DPSK receiver, DS-BPSK receiver has been used as the reference receiver in this thesis. The BER comparison is considered as our base to confirm the practicality of the proposed DS-DPSK receiver.

1.3 Thesis Organization

This thesis is organized as in the following. Chapter 2 presents a thorough background material on UWB technology. Chapter 3 introduces CDMA technology and its use in the context of UWB. Chapter 4 defines and represents the proposed DS-DPSK system mathematically. In addition, it provides all the associated analytical derivations for the receiving device and its average probability of error. The simulation approach and the associated simulation results for both systems DS-DPSK (proposed) and DS-BPSK (reference) are presented in Chapter 5. Finally, the conclusion is presented in Chapter 6.

CHAPTER 2

BACKGROUND ON UWB

2.1 History of UWB

UWB is an old technology which was first employed by Guglielmo Marconi in 1901 to transmit Morse code sequences across the Atlantic Ocean, using spark gap radio transmitters. After that period, approximately 50 years ahead, this technology was restricted to military applications, especially in impulse-radars applications and was classified as highly secured communications [20]. In 2002, the federal communications commission (FCC) in USA has realized the unique properties of UWB technology, especially with the recent advancement in semiconductor and VLSI technologies. A group of industry leaders, who's interested by the development of UWB technology, have placed immense pressure on the FCC to approve UWB technology for commercial use. As a result, the FCC has released the First Report and Order for commercializing UWB technology in February 14, 2002. In this report, the FCC has defined the allocated spectrum and the associated restricted operating conditions for this new technology.

2.2 UWB Definition

The FCC has assigned UWB communication systems a broad range of unlicensed (free) frequency spectrum that extends from 3.1-10.6 GHz. Based on the FCC definition, UWB signal during transmission should have instantaneous radio with a fractional bandwidth greater than 20% or bandwidth greater than 500MHz [21]. Fractional bandwidth (f_B) is the metric that always used to classify communication signals as narrowband, wideband or ultra-wideband signals. In the context of UWB, the fractional bandwidth mathematically defined as

$$f_B = \frac{BW}{f_c} * 100\% = \frac{2(f_h - f_l)}{f_h + f_l} * 100\% \ . \tag{2.1}$$

Fractional bandwidth is the percentage ratio of the bandwidth to center frequency. The bandwidth defined as the difference between -10 dB cut-off frequencies from the spectral peak-power value of UWB signal. The spectral power graph represents the power contents of UWB signal at different frequencies within its frequency domain representation.

The shape of the propagation radio in UWB communication systems during the transmission of the information bits, determines whether these systems are designed based on the single-band approach or the multi-band approach.

2.2.1 Single-band Approach

This approach is based on the original idea of UWB, which is called the Impulse-Radio transmission technique. The idea is to use of an extremely short-duration pulse of a nanosecond order or less, that spread its energy (or power) over a huge range of frequencies within the available UWB spectrum with very low power spectral density. Therefore the bandwidth of this pulse is instantaneous and occupy a large portion of the available UWB spectrum, if not the whole spectrum. Figure 2.1 depicts occupied instantaneous bandwidth based on the single-band approach.

In literature, systems designed based on this approach are known as IR-UWB communication systems. The main supporters for this idea are Motorola/XtremeSpectrum and

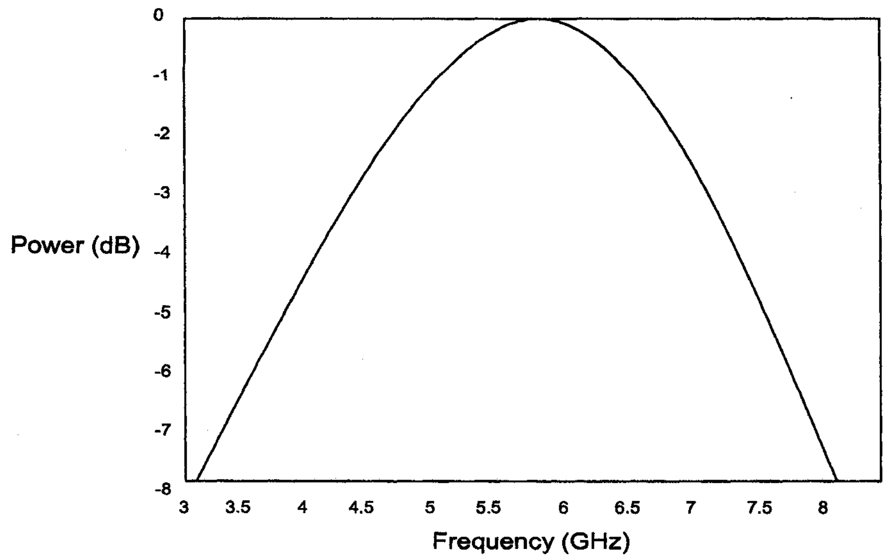

Figure 2.1: Single-band Approach

Freescale Semiconductor - both are industry leaders, in addition to some other supporters all joined together under **UWB Forum**. Gaussian pulse and its derivatives are widely used in studying and analyzing wireless communication systems proposed based on IR-UWB idea because of their simplicity and mathematical tractability. In addition to Gaussian pulse and its derivatives, there are many short-duration pulses that exist in literature such as chirp, hermite-based and wavelet pulses.

2.2.2 Multi-band Approach

In this approach, the available UWB spectrum is divided into several non-overlapping sub-bands. Multiple carrier signals, each centered at individual sub-band, are used to modulate a short-duration pulse in simultaneous manner. Each of the short-duration pulses has an instantaneous bandwidth greater than 500MHz to follow the FCC definition of UWB signal. Figure 2.2 depicts the division for UWB spectrum based on multi-band approach.

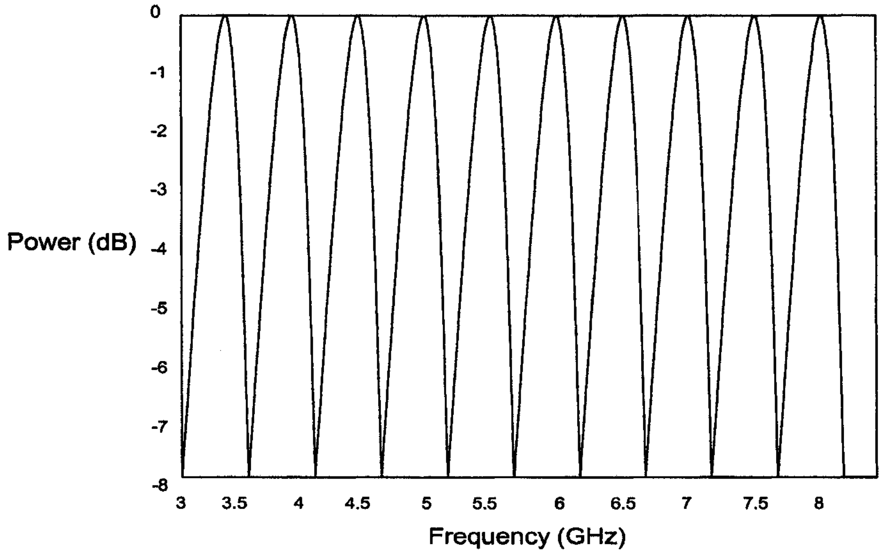

Figure 2.2: Multi-band Approach

In literature, systems designed based on this approach are known as MC-UWB communication systems. The main supporters for this idea are Intel and Phillips - both are industry leaders, in addition to some other supporters all joined together under **Wimedia Alliance**. Gaussian pulse, its derivatives and the other existing short-duration pulses, are also used to study and analyze UWB communication systems proposed based on multi-band idea, except that the pulses are not as narrow as the pulses used in the single-band approach.

2.3 Standardization

The emergence of UWB technology was the main reason for the formation of task group 3a (TG3a), which is one of the already defined functional task groups under IEEE 802.15 WPAN working group. TG3a main responsibility was to define an alternative-physical (Alt-PHY) layer using UWB technology for the 4G WPAN communication systems. It is intended to replace the already existing Physical Layer defined under IEEE 802.15.3 standard. The selection criterion for UWB as an alternative-physical layer technology for the previous standard is based on its unique properties those satisfy the requirements of 4G wireless communication systems.

Standardization process was initially conducted under the supervision of TG3a. TG3a final goal was to perform the down selection from many proposals submitted to them for compiling the new WPAN physical layer standard, namely IEEE 802.15.3a, from the winning proposal. Functional task groups currently defined under IEEE 802.15 working group are shown in Figure 2.3.

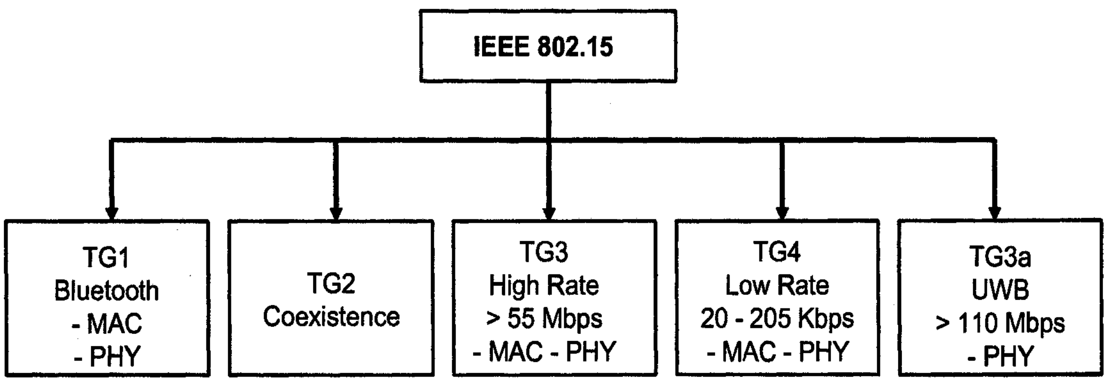

Figure 2.3: Current Task Groups Defined Under IEEE 802.15 Working Group

Unfortunately, the process of coming up with the new standard by TG3a has essentially come to a deadlock [22]. This is because the remaining two proposals after the down selection process, namely MBOA proposal [23] which is based on the multi-band approach and DS-UWB proposal [24] which is based on the single-band approach, have an equal weight in terms of their supporters, technical credibility, and impression.

TG3a currently has relegated the control of standardization process to Wimedia Alliance and UWB Forum. Industry leaders in both groups are currently designing UWB communication systems based on their respective approach and are feeding the current wireless market by these systems. The market will decide on the winning approach by observing the most sellable UWB systems for consumers segment.

2.4 Regulations

UWB is an overlay technology that should coexist with other licensed radio services, such as global positioning systems (GPS), north american GSM service (PCS), industrial scientific medical band services (ISM), and UNII service (802.11a) as shown in Figure 2.4.

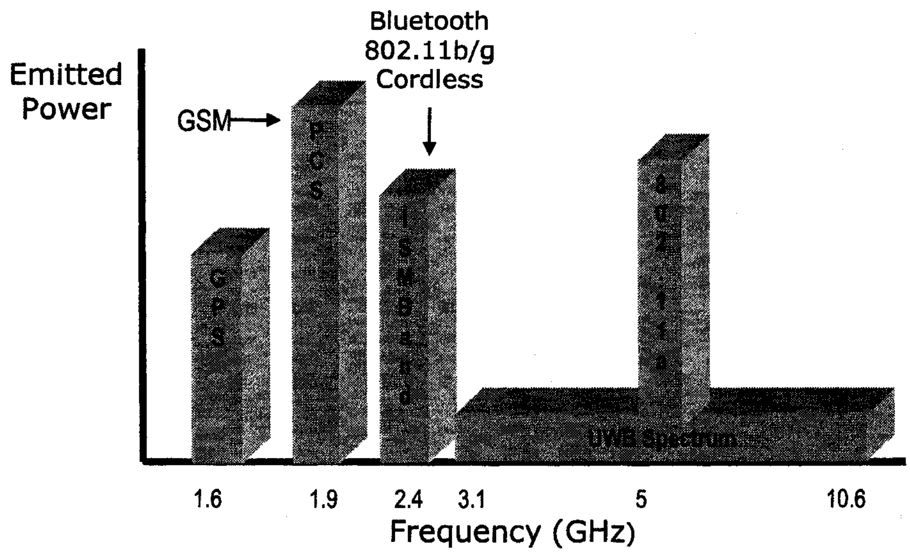

Figure 2.4: UWB is an Overlay Technology

The possibility of UWB signal to interfere with the signals of other existing licensed radio services is the main concern for the manufacturers of these services. Therefore, to ensure the minimum level of interference, FCC has defined a severe spectral mask on UWB signal during its transmission. The maximum allowed power spectral density for UWB signal as defined by the FCC regulations is -41.3 dBm/MHz, which is equivalent to 75 nW/MHz in linear scale [25].

The FCC has categorized UWB systems based on their intended applications into three main categories: communication systems, imaging systems, and vehicular radar systems. UWB communication systems are subdivided further into the indoor and outdoor systems. Figure 2.5 depicts the restrictive spectral mask imposed by the FCC on UWB signal during its transmission in indoor and outdoor communication systems.

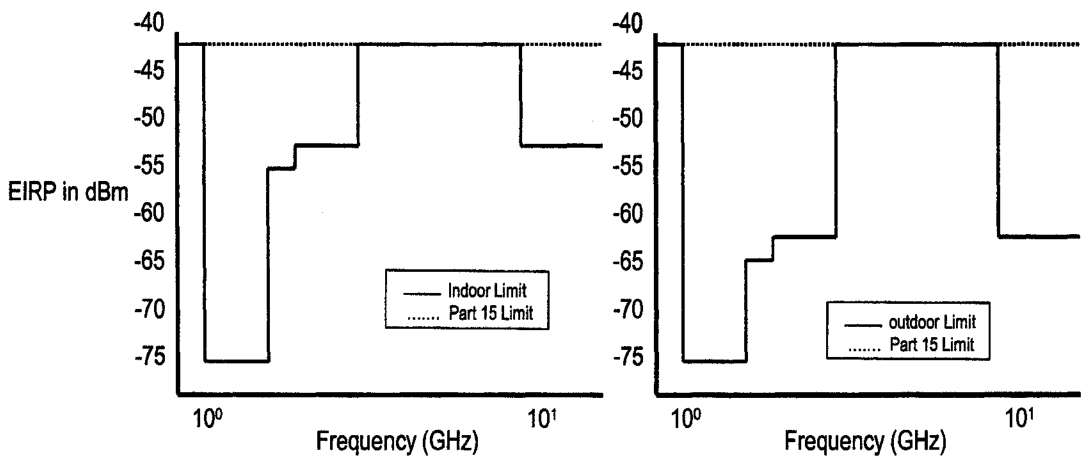

Figure 2.5: Spectral Mask for UWB Communication Systems

Referring to Figure 2.5, the imposed spectral mask on UWB signal in UWB indoor communication systems is 10dB higher than that imposed in UWB outdoor communication systems within 1.61 - 3.1 GHz band. This further limitation on the transmission of UWB signal in outdoor devices is aimed to protect PCS, GPS and ISM band systems from the possible interference of UWB signal.

2.5 Challenges

UWB technology is not all about advantages, hence there are some associated challenges with this new technology that should be addressed [26]. Most of these challenges are the result of using ultra short-duration pulse for transmission. Some known challenges associated with this technology are listed below:

- All sources of noise and interference on short-duration pulses exacerbate the detection process, and
- Severe power restrictions on short-duration pulses make UWB systems vulnerable to timing errors and jitter, and
- The requirement for very fast analog to digital converters (speed of few GHzs) to sample and synchronize the stream of pulses at receiver side, and
- Pulse shape distortion as a result of using extremely short-duration pulses with low energy and power contents make the channel estimation a difficult task.

2.6 Chapter Summary

In this chapter, the relevant background material on UWB technology has been presented in simple way. Although impulse-radio UWB is an old invention, since Guglielmo Marconi in 1901, at that time the unique characteristics of IR-UWB signal like the large bandwidth and spectrum sharing for MA support were not fully utilized.

Since commercializing this technology, the FCC has defined all the associated regulations and operating conditions to assure the minimum interference effect of this free-of-charge technology on other licensed services. The current prevalence of IR-UWB communication systems in literature is the result of addressing and utilizing the unique characteristics of that old invention.

IR-UWB communication systems are characterized by their simplicity because their transceivers do not require complex signal processing modules, such as the Fourier transform and its inverse. IR-UWB communication systems are capable of supporting high data rates because they utilize extremely short-duration pulses in time. Due to their restricted power spectral density transmission levels, IR-UWB systems can coexist with other radio services and share the available spectrum for MA support.

CHAPTER 3

CDMA CONCEPTS IN IR-UWB

3.1 CDMA Technology

To provide a multiple-access environment, where many active-users can transmit their information bits simultaneously, with the ability to recognize a specific active-user of interest, which is currently sending its information bits within the system under consideration, any of the well-known traditional channel accessing schemes has to be utilized. Such schemes are time division multiple-access (TDMA), frequency division multiple-access (FDMA), and code division multiple-access (CDMA). This section will introduce CDMA technology, which is the channel accessing scheme of choice in this work, along with its associated protocols. CDMA technology in conjunction with spread spectrum concepts are widely used in the context of wireless cellular technology [27].

3.1.1 CDMA Definition

Code division multiple-access (CDMA) is a channel accessing scheme that permits MA capability for many active-users within the system under consideration by means of coding. In this scheme, each active-user is assigned a unique pseudo-noise (PN) code sequence during its transmission. The shift register that is used to generate these code sequences in the transmitter automatically generates different PN code sequences for different active-users. In this scheme, it is always assumed that the receiver already knows the unique code sequence of the desired user currently sending its information bits. In this case, the receiver will be capable of detecting the transmitted information bits after decoding (or despread) using the correlator, which relies on the PN code generator module to generate the desired code sequence [28].

3.1.2 CDMA Protocols

CDMA protocols consist of a collection of protocols, where they are distinguished from each other through the way they reduce the available interference, and through the way they modulate (or encode) the information bits that are ready for transmission. Classifying CDMA protocols based on the way of reducing the available interference provides the averaging systems and the avoidance systems. In averaging systems the interference is reduced by averaging it over a long time interval. In avoidance systems the interference is reduced by avoiding it for a large portion of time. Classifying CDMA protocols based on the used modulation (or encoding) scheme provides a collection of protocols such as direct-sequence protocol, frequency-hopping protocol, time-hopping protocol, chirp spread-spectrum protocol, and the hybrid protocol [29]. Wireless communication systems employing any of the aforementioned protocols are classified as avoidance systems, except for these systems employing the direct-sequence CDMA protocol. Direct-sequence CDMA protocol is an averaging system that has been used in this work.

3.2 Concepts of Spread-Spectrum

To allow for concurrent spectrum-sharing among multiple active-users within the available spectrum of a specific wireless technology under consideration, for long time, spread-spectrum multiple-access (or CDMA) protocols came into play to achieve this goal. In general, the final goal of the traditional spread spectrum protocols, such as the use of DS-CDMA protocol in narrowband and wideband systems, is to guarantee that the transmission signal has a very low power spectral density while extending its energy contents over a broad bandwidth. The power spectral density is the signal's power contents in frequency domain. In this case, multiple active-users can coexist with each other and share the available spectrum, where the interference is guaranteed to be at its minimum levels.

This section defines the traditional spread-spectrum technique based on DS-CDMA protocol, which is widely used in narrowband and wideband communication systems, especially those systems designed for wireless local area networks (WLANs) and wireless cellular applications. This section then highlights the differences between the traditional spread-spectrum techniques and the inherent spread-spectrum of IR-UWB pulse. In addition it exhibits the usage of DS-CDMA protocol in the context of UWB.

3.2.1 Spread-Spectrum and IR-UWB

In conventional spread-spectrum systems, such as the use of direct-sequence spread spectrum multiple-access (DS-SSMA or DS-CDMA) protocol in narrowband and wideband systems, spreading the spectrum is achieved by changing the frequency of the information signal [30]. In this scheme, a high frequency signal, called the chipping or coding signal, that has a higher frequency than the information signal is directly multiplied by the information signal to expand (or spread) its energy over a broad frequency range. This direct multiplication (or encoding) converts the information signal into a transmission signal, which has a much broader bandwidth than the information bandwidth. Figure 3.1 depicts the idea of spreading the spectrum using DS-CDMA protocol that is used in narrowband and wideband systems.

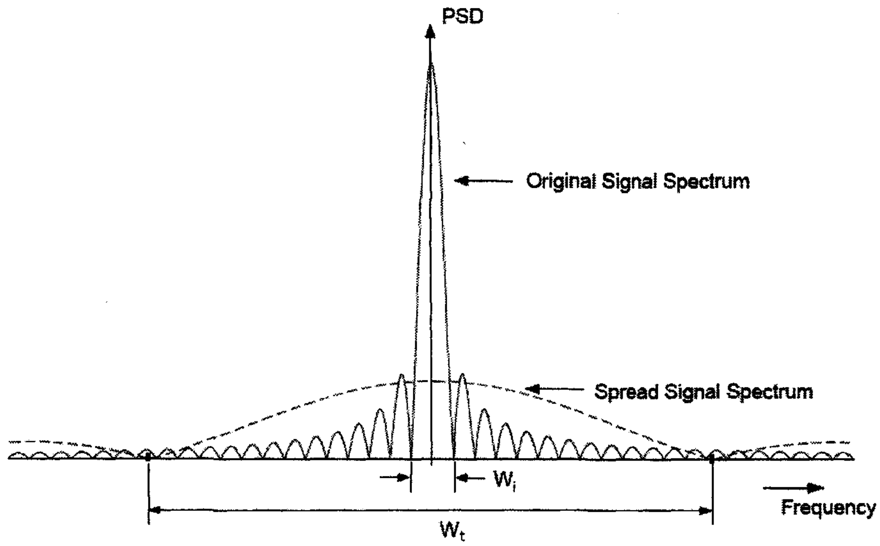

Figure 3.1: Spread-Scpectrum Concept in Traditional Systems

The amount by which the information signal is spread depends on the processing gain factor. The processing gain (PG) mathematically defined as

$$PG = \frac{W_t}{W_i}, \tag{3.1}$$

where W_t is the transmission bandwidth and W_i is the information bandwidth. These parameters are depicted visually in Figure 3.1. For higher processing gain values, the transmission bandwidth is getting broader; consequently the power spectral density of the transmitted signal is getting lower.

In contrast, spreading the spectrum in IR-UWB is achieved through the use of an extremely short-duration pulses that has a huge swath of frequency band within the available UWB spectrum. This type of spreading the spectrum is called temporal spreading, because the time-shortness for the employed pulse is the main factor for spreading the energy of the transmitted signal [31]. Because the employed pulse is in the nanosecond order or even less, the bandwidth of the transmission signal will be in the range of few GHzs. In addition the power spectral density of the transmission signal is extremely low and even below the noise floor of other radio technologies.

3.2.2 DS-CDMA and IR-UWB

In IR-UWB communication systems each information bit to be transmitted is represented by a specific number of IR-UWB pulses. Therefore, a random stream of binary data bits is nothing more than a random stream of binary IR-UWB pulses transmitted in sequence. This stream has a specific rate determined by the pulse repetition period. For any IR-UWB communication system that is employing the DS-CDMA protocol, if the pulse repetition period of IR-UWB stream is equal to the period of the used pseudo-noise (PN) code sequence, and the number of pulses per data bit is equal to the length of the used PN code sequence, then the periodic PN code sequence will repeat itself every bit period. Therefore, when the utilized unique PN code sequence is multiplied by the stream of IR-UWB pulses it will amplitude-modulate these pulses periodically based on the sign of its constituent code elements. From the above discussion, the main idea of using DS-CDMA protocol in the context of IR-UWB is not to spread the information bandwidth, but to periodically amplitude-modulate the random stream of IR-UWB pulses for each active-user, hence differentiating active-users for multiple-access (MA) support [32].

In CDMA technology and its associated protocols, such as DS-CDMA protocol, the employed PN code sequences are random, but they are periodic. Because they are random they have noise-like properties, which means that they are independent of each other and have the minimum possible interference among each other. Therefore, they are suitable for supporting MA environments because they are capable of differentiating active-users and producing the minimum interference. Depending on the configuration and the length of the shift register, the underlying PN code sequences generator will produce a different set of PN code sequences, each with unique and distinct properties. In CDMA literature, some of the known PN code sequences are the Walsh Hadamard code sequences, Kasami code sequences, Maximum Length code sequences, and Gold code sequences [33].

Gold code sequences are used in this work because of their superior properties those are suitable for MA support. The most important property represented by their ability to improve the receiving device BER performance, as they have the minimum possible interference among each other (they are semi-orthogonal codes). Another good reason for using the gold code sequences is to match the parameters of the reference system. The other attractive properties of the gold code sequences are explained in subsequent chapters of this thesis.

3.3 Practical DS-CDMA Receivers

The practical direct-sequence code division multiple-access (DS-CDMA) receiver for multiple-access (MA) support mainly consists of two modules, namely the demodulator and the correlator [34]. The used modulation scheme at the transmitter determines the type of the above DS-CDMA receiver. The practical DS-CDMA receivers for IR-UWB communication systems can be classified either as coherent or noncoherent.

In one hand, if a noncoherent modulation scheme such as the differential phase-shift keying (DPSK) is employed at the transmitter, the receiver should implements a noncoherent demodulation scheme to recover the transmitted information bits. In this case, the receiver is considered as a noncoherent device, and the entire IR-UWB communication system is considered as a noncoherent system.

On the other hand, if a coherent modulation scheme such as the binary phase-shift keying (BPSK) is employed at the transmitter, the receiver should implements a coherent demodulation to recover the transmitted information bits. In this case, the receiver is considered as a coherent device, and the entire IR-UWB communication system is considered as a coherent system.

3.3.1 Noncoherent DS-CDMA Receiver

In DPSK modulation, the transmitted bit is included within the phase-transitions of the carrier signal. Therefore the demodulator does not need the carrier for demodulation. In this case, the template signal necessary for demodulation is represented by the previous signaling interval of the carrier signal, which has a single bit-period (T_b) duration. This signal can be used to recover the transmitted bit by comparing its phase with the phase of the current signaling interval of the carrier signal. Depending on the result of this comparison the transmitted bits are recovered [35]. A practical DS-CDMA receiver for IR-UWB communication systems that employs DPSK modulation and supports multiple-access is shown in Figure 3.2. As shown in that figure, the template signal necessary for demodulation in this receiver is the delayed-replica (delayed by one bit-period) of the received signal itself. This detection scheme in literature is known as the bit-level differential-detection. Hence the receiver shown in Figure 3.2 is referred to as the differential-detector. The simplicity of this receiver is the main advantage, but its suboptimum BER performance is the main dis-

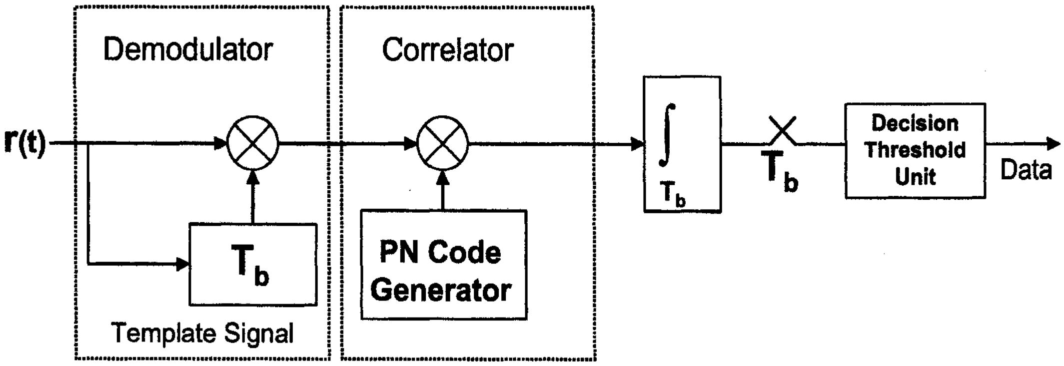

Figure 3.2: DPSK-Based Direct-Sequence Receiver (noncoherent)

advantage. The receiver shown in Figure 3.2 is known to have the worst BER performance within the class of differential-detectors [34].

3.3.2 Coherent DS-CDMA Receiver

In BPSK modulation, the transmitted bit is included within the phase itself of the carrier signal. Therefore the demodulator does need the phase of the carrier to assist in the demodulation. A carrier recovery circuit is necessary for tracking and extracting the carrier-phase from the received signal [35]. In the demodulator, the reference signal that matches the originally transmitted signal, when multiplied by the recovered carrier-phase will produce the locally generated template (LGT) signal, which performs the demodulation with the received signal and recovers the transmitted bits. A practical DS-CDMA receiver for IR-UWB communication systems that employs BPSK modulation and supports multiple-access is shown in Figure 3.3. As shown in that figure, the additional components necessary for coherent demodulation, such as the carrier recovery circuit, the analog multiplier and the reference signal adds design complexity for BPSK-based direct-sequence receiver. This implies extra costs and power consumption compared to DPSK-based direct-sequence re-

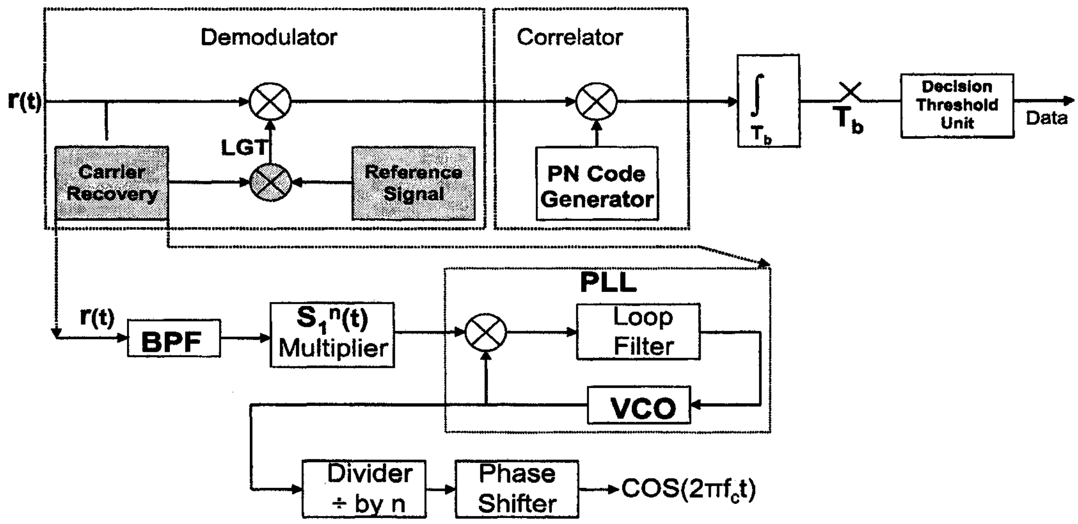

Figure 3.3: BPSK-Based Direct-Sequence Receiver (coherent)

ceiver. In return, the BER performance of BPSK-based direct-sequence receiver is better than that of DPSK-based direct-sequence receiver. This is due to its ability to capture and track the exact phase using the carrier recovery circuit, and due to the existence of only a single noise-term during the demodulation. In contrast, DPSK-based direct-sequence receiver is less complex from design perspective; however, its BER performance is degraded as a result of using the noisy template, which results in two noise-terms during the demodulation [36]. Coherent receivers are always suffer from phase ambiguity (or phase reversal) of 180 degrees as a result of using the carrier recovery circuit. If this ambiguity is not corrected, the system BER performance is drastically degraded. Phase ambiguity problem does not exist in DPSK-based direct-sequence receivers [37].

3.3.3 Other Considerations

In multi-path fading channels, the scattered replicas of the transmitted pulse are the dominating channel effects. Rake receivers are designed specifically to collect the energy from the scattered multi-path components [38, 39]. Coherent modulation such as BPSK permits the use of coherent-rake receivers, also known as selective-rake (S-Rake) receivers. S-Rake receivers require full channel estimation, necessary to capture and track the amplitude, delay and phase of scattered components. In addition, S-Rake receivers should implement the selection diversity necessary to combine the collected energy, such that to maximize the signal-to-noise ratio (SNR) metric, therefore, they are complex in their design and consume extra power.

Alternatively, noncoherent modulation such as DPSK permits the use of noncoherent-rake receivers, also known as partial-rake (P-Rake) receivers. P-Rake receivers do not require full channel estimation and selection diversity, and collect only the energy of a specific number of scattered components based on their sequence of arrival. Those receivers are simple in their design and consume less power [40]. There are some situations in which the estimation of the multi-path fading channel is difficult and cumbersome. In these cases, the solution is to use DPSK modulation combined with differential-detection for the same compelling reasons as mentioned above [41].

The proposed receiver works based on the differential-detection scheme that previously explained and used by the receiver shown in Figure 3.2. The structure of the proposed receiver has a different configuration when compared to that receiver structure, but with a comparable complexity when considering the constituent components of both receivers. The proposed receiver can acquire time synchronization with the received signal, but not phase synchronization. Therefore, its BER performance should be better than that for the receiver shown in Figure 3.2, which is known to have the worst BER performance as mentioned previously.

3.4 Chapter Summary

In this chapter, the relevant background material on CDMA technology, its associated spread-spectrum protocols and its use in the context of UWB technology, especially in IR-UWB communication systems, was presented in interesting way. Based on the way of reducing the available interference, CDMA spread-spectrum protocols were classified either as averaging or avoidance systems. The protocol of interest in this work is the direct-sequence CDMA protocol, which is also known as the direct-sequence spread spectrum multiple-access protocol.

DS-CDMA protocol is an averaging system that averages the interference over a long time interval. The data bits in any communications system employing direct-sequence CDMA protocol are directly modulated based on the sign of the utilized PN code sequence. Direct-sequence CDMA protocol has been used widely in narrowband and wideband wireless communication systems, but its usage in the context of IR-UWB communication systems is slightly different. This chapter has defined the difference between spreading the spectrum in the traditional communication systems with that in IR-UWB communication systems.

The differences between coherent and noncoherent IR-UWB receivers those designed for MA support were also covered in this chapter. Despite their optimal BER performance relative to noncoherent receivers, coherent receivers are considered complex from design perspective, because they need carrier recovery circuit and full channel estimation. Alternatively, noncoherent receivers are simple from design perspective, but their BER performance is inferior up to 3dBs.

As previously stated in this chapter, the primary concerns for proposing our noncoherent DS-DPSK receiver are to trade-off the slight BER performance degradation with simple receiver structure, that is capable of relaxing the carrier recovery circuit and the full channel estimation, in the mean time, to avoid the phase ambiguity problem which is inherent in coherent receivers, therefore, the proposed noncoherent IR-UWB receiver structure is expected to have less costs and power consumption.

CHAPTER 4

THE PROPOSED IR-UWB RECEIVER

4.1 Introduction

This chapter is dedicated to define and represent the proposed system mathematically. In addition, it provides all the associated analytical derivations for the proposed receiver and its average probability of error. The general situation for the problem under consideration is represented by the ability to find a novel receiver, that has a simple structure with a relatively good performance, which can detects the random stream of simultaneous IR-UWB pulses transmitted by many active-users within the system, while taking into account the channel effects such as the multiple-access interference and the unavoidable receiver noise. The general environment that best describes the above situation is illustrated in Figure 4.1.

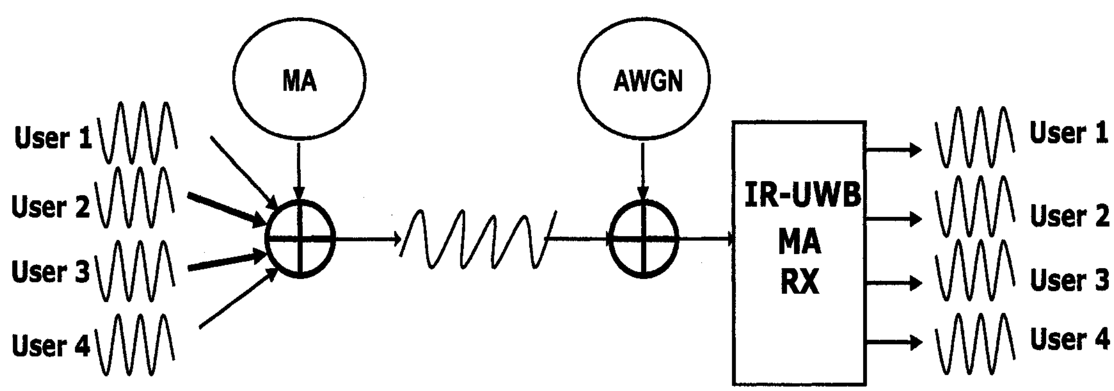

Figure 4.1: General Environment under Considerstion

In this chapter a novel IR-UWB receiver which is intended to solve the abovementioned problem is proposed. The complete system consists of three main modules, namely the transmitter, the channel and the receiver. In this system, the transmitter employs the noncoherent bit-level DPSK modulation combined with DS-CDMA to differentiate active-users for MA support. Because multiple active-users can transmit simultaneously, this system will be investigated under the channel effect that includes both the multiple-access interference (MAI) and the unavoidable receiver noise. In this system, the noncoherent IR-UWB receiver can detect the transmitted information bits of many active-users transmitting their data concurrently while experiencing the channel effects. Because of DS-CDMA and DPSK modulation, the proposed system is referred to as DS-DPSK.

The following section in this chapter defines and presents the proposed DS-DPSK system mathematically. The main modules in this system are described mathematically based on their constituent components. The analyses in the rest of this chapter are divided into two main sections, namely receiver and probability of error analysis. In receiver analysis section, all the associated statistics with the receiving device are analyzed to come up with the corresponding mathematical expressions that are used in the subsequent section. In probability of error analysis section, the derivation process for the final expression for the average probability of error of the proposed receiver is presented. The derived analytical expression is used for BER performance comparisons in later chapters. A brief summary is provided at the end of this chapter aimed to highlight the main points covered in this chapter.

4.2 Proposed DS-DPSK System Model

Figure 4.2 depicts the complete block diagram for the proposed DS-DPSK system.

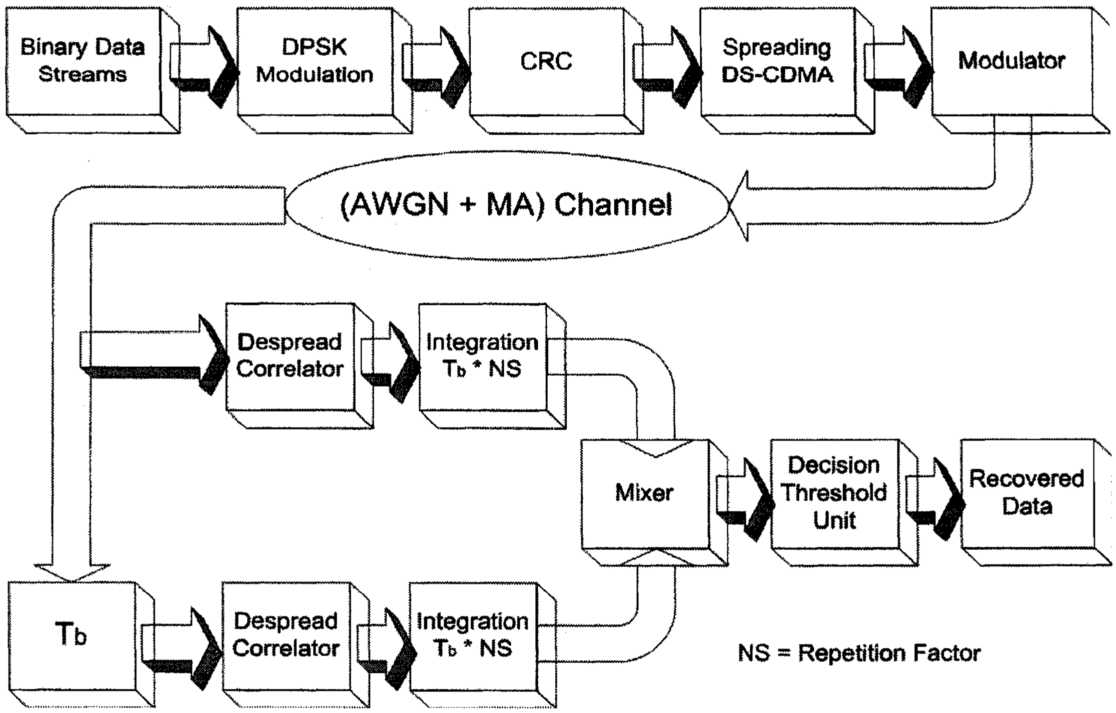

Figure 4.2: Proposed DS-DPSK System

Before describing the constituent modules of the proposed system mathematically, there are some assumptions those were considered during the simulation phase for this system. These assumptions have a direct influence on the derived analytical expression for the average probability of error in the proposed receiver of this system. Therefore, these assumptions should be addressed at the very beginning as in the following:

- The transmitted signal is normalized such that the energy per data-bit is unity, and
- The system is synchronous, which means that all users are synchronized in time at the receiver input, and
- When despread, the receiver can acquire time synchronization with the received waveform, but not phase synchronization, and

- The inherent Near-Far problem in CDMA channels is not exist, since all users at the receiver input are assumed to have the same power (i.e., perfect power control is assumed).

The following three subsections presents the mathematical descriptions for each of the constituent modules of the proposed system individually. The obtained expressions will assist in understanding the functional aspects of the proposed system. In addition, they will assist in deriving the final analytical expression for the average probability of error in the proposed receiver.

4.2.1 Proposed DS-DPSK Transmitter

The transmitter of the proposed system (DS-DPSK) consists of five components as shown in the following block diagram in Figure 4.3.

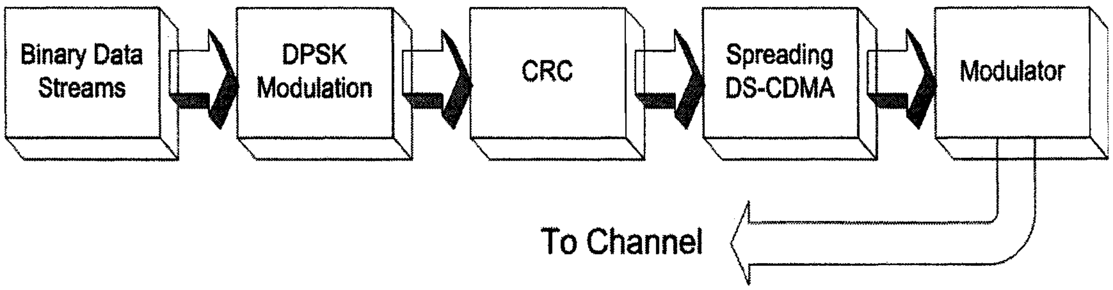

Figure 4.3: The Proposed DS-DPSK Transmitter

- Binary Data Streams: Represents the information bits, where they are independent and identically distributed (i.i.d) random binary sequences. They are equally probable with bipolar non-return-to-zero (NRZ) line coding which belongs to {-1,1}.

- DPSK Modulation: Includes the information bits within the phase-transitions of the transmitted signal by following the same procedure as shown in Figure 4.4.

Msg Sig		1	-1	1	1	-1	-1	1	1	1
DPSK Sig	1	1	-1	-1	-1	1	-1	-1	-1	-1

Figure 4.4: DPSK Modulation

In this scheme, it is always assumed that there is a leading binary bit '1' in DPSK Sig to be transmitted, which acts as the reference bit at receiver side. Then, if the coming data bit in the Msg Sig is the binary bit '1', set the current bit the same as the previous bit in DPSK Sig to be transmitted. Otherwise, if the coming data bit in the Msg Sig is the binary bit '0', toggle the current bit with respect to previous bit in DPSK Sig to be transmitted.

- Code Repetition Coder (CRC): Represents a simple forward error correction (FEC) scheme for BER performance improvement. When $NS = 1$, where NS is the repetition factor, then CRC scheme is not supported.

- Spreading/DS-CDMA: In this component, each information bit is represented by a specific number of IR-UWB pulses (let's say N_c pulses per data bit). DS-CDMA protocol is used to amplitude-modulate the transmitted stream of IR-UWB pulses, those belong to the transmitted information bits of a specific active-user, using the sign of the constituent code elements of the utilized Gold code sequence. The Gold code sequences behave like noise because they are pseudo-noise codes, but they are deterministic. Therefore, they have excellent properties that can be used for supporting multiple-access environments [29] such as:

- Balance Property: Gold code sequences have equal number of 1's and 0's to eliminate the effect of the DC component. Good for spectral smoothening, and
- Auto-correlation Property: Gold code sequences have a large peak value at time equal to zero when correlated with themselves. Good for receiver timing and synchronization, and
- Cross-correlation Property: Gold code sequences have very low interference contribution among each other, where they are semi-orthogonal codes. Good for minimum MAI effect in multiple-access environments, and
- Maximum Users Support Property: Gold code sequences generated from the preferred pairs of m-sequences, which allow them to have large set of codes with excellent properties for supporting a large number of active-users in the system.

• Modulator: The square pulses at the output of Spreading/DS-CDMA component are mapped to the 2^{nd} derivative Gaussian pulses. The frequency contents of these pulses are shifted to the appropriate frequency band using this component.

The transmitter of DS-DPSK system is similar to that of the reference DS-BPSK system which is shown above in Figure 1.1, except that the information bits are bit-level DPSK modulated. Because of DPSK modulation and DS-CDMA spreading, the transmit signal of DS-DPSK system for the k^{th} user is given by

$$S_{tr}^{(k)} = \sum_{j=-\infty}^{\infty} \sum_{n=0}^{N_c-1} d_j^{(k)} c_n^{(k)} p_{tr}(t - jT_b - nT_c) \ , \tag{4.1}$$

where $d_j^{(k)} = d_{j-1}^{(k)} b_j^{(k)} \ \forall \ b_j^{(k)} \in \{-1, 1\}$ is the j^{th} DPSK modulated bit, $c_n^{(k)}$ is the used gold code sequence, $p_{tr}(t)$ is the transmitted 2^{nd}derivative Gaussian pulse, T_c is the pulse repetition period, N_c is the number of pulses per bit and the bit period is $T_b = N_c * T_c$. Figure 4.5 depicts the shape of the transmit signal at the output of the transmitter.

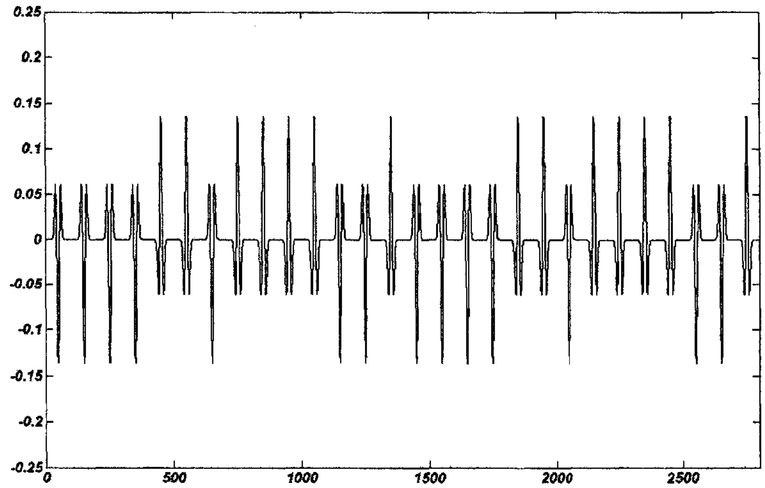

Figure 4.5: Transmit Signal in DS-DPSK System

The transmitted signal has a low-valued amplitude as a result of energy normalization and experience no randomness in amplitude because the channel effect is not yet considered.

4.2.2 Proposed DS-DPSK Channel

The channel is the additive white Gaussian noise (AWGN) with multiple-access channel that has two sources of noise, namely:

- Receiver noise, $n(t)$: represented by the additive random noise at receiver input.

- Multiple-access interference, MAI: represented by the aggregate effect of having more than one active-user in the system simultaneously.

Receiver noise, $n(t)$, modeled as a white Gaussian random process with zero-mean and variance σ_n^2, i.e., $N(0, \sigma_n^2)$. The receiver noise modeled such that to have a two-sided power spectral density equal to $N_o/2$. The multiple-access interference, MAI, effect approximated as a white Gaussian random process. Figure 4.6 depicts the shape of the received signal after experiencing the channel effects.

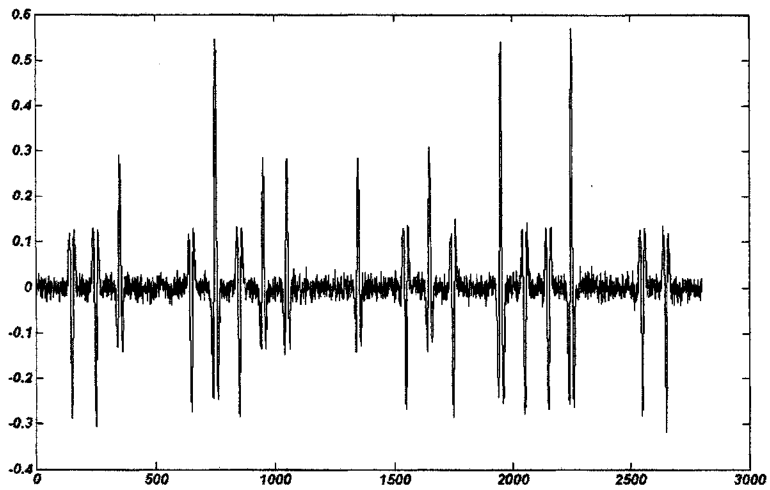

Figure 4.6: Received Signal in DS-DPSK System

As shown in Figure 4.6, the channel effect is represented by the addition of the random noise which is apparent from the random fluctuations in the amplitude of the received signal, and the increase in the amplitude at specific points of the received signal as a result of MAI effect.

4.2.3 Proposed DS-DPSK Receiver

When there are N_u active-users in the system, the received signal can be expressed as

$$r(t) = \sum_{k=1}^{N_u} S_{rec}^{(k)}(t) + n(t) \ , \tag{4.2}$$

where $S_{rec}^{(k)}(t)$ is the received signal of k^{th} user at receiver input, and $n(t)$ is the added receiver noise.

Bit-level DPSK modulation at transmitter side allows for bit-level differential-detection at receiver side. In this scheme, the previous signaling interval (i.e., bit-period long) is used to recover the originally transmitted data bit from the current signaling interval. Therefore, the proposed receiver should have two branches, namely branch A and B, to represent $r(t)$ and $r(t - T_b)$ as shown in Figure 4.7.

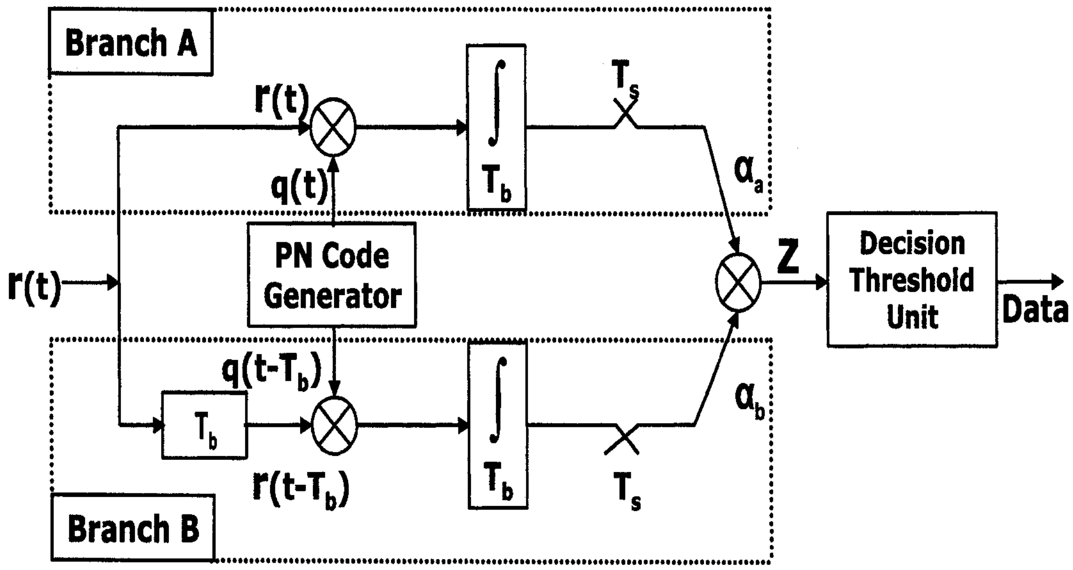

Figure 4.7: The Proposed DS-DPSK Receiver

At receiver input each active-user is recognized by a unique pseudo-noise (PN) code. The PN code generator which is shown in Figure 4.7 exists mainly to generate the unique code sequence for the active-user who is currently receiving its information bits. The variable statistics at each branch, namely α_a and α_b, are the result of correlating $r(t)$ and $r(t-T_b)$ with the desired-user PN code sequence over bit-period. Multiplying α_a and α_b is equivalent to extracting the sign or the phase-difference between the current and previous signaling intervals. The decision statistic, Z, at the mixer-output is then compared against the threshold to recover the transmitted information bit.

4.3 DS-DPSK Receiver Analysis

In this section, the variable statistics, namely α_a and α_b, and the decision statistic Z those are shown in Figure 4.7 are analyzed, and expressed mathematically. The analytical expression for the average probability of error of the proposed receiver will be derived.

4.3.1 DS-DPSK Receiver - Branch A

The correlator output in Figure 4.7 is given by

$$\alpha_a = \int_0^{T_b} r(t)q(t)dt \ . \tag{4.3}$$

The assumption hereafter is that user 1 currently receiving data, and the l^{th} data bit will be detected. In this case, the despread signal out of the PN code generator module is expressed as

$$q(t) = \sum_{m=0}^{N_c-1} c_m^{(1)} p_{rec}(t - lT_b - mT_c) \ , \tag{4.4}$$

and the received signal after simplification is expressed as

$$r(t) = \sum_{n=0}^{N_c-1} d_l^{(1)} c_n^{(1)} p_{rec}(t - lT_b - nT_c) + n_s \ , \tag{4.5}$$

where $n_s = \sum_{k=2}^{N_u} S_{rec}^{(k)}(t) + n(t)$ is the noise source at branch A including MAI and receiver noise $n(t)$, and excluding the signal of the desired user. $S_{rec}^{(k)}(t)$ is the received signal of k^{th} user at receiver input. Using Equation (4.3), α_a at the l^{th} data bit is defined as

$$\alpha_a = \int_0^{T_b} \left\{ \sum_{n=0}^{N_c-1} d_l^{(1)} c_n^{(1)} p_{rec}(t - nT_c) + n_s \right\} * \sum_{m=0}^{N_c-1} c_m^{(1)} p_{rec}(t - mT_c) dt \ . \tag{4.6}$$

Let $\alpha_a = m_a + n_a$, where m_a and n_a are the desired signal and the noise source components at branch A. The desired signal component m_a is defined as

$$m_a = \int_0^{T_b} \sum_{n=0}^{N_c-1} d_l^{(1)} c_n^{(1)} p_{rec}(t - nT_c) \ * \sum_{m=0}^{N_c-1} c_m^{(1)} p_{rec}(t - mT_c) dt = N_c E_p d_l^{(1)} = E_b d_l^{(1)} \ , \tag{4.7}$$

and the noise component n_a is defined as

$$n_a = \int_0^{Tb} n_s * \sum_{m=0}^{N_c-1} c_m^{(1)} p_{rec}(t - mT_c) dt \ . \tag{4.8}$$

Therefore n_a can be expressed as

$$n_a = \int_0^{Tb} \left\{ \sum_{k=2}^{N_u} S_{rec}^{(k)}(t) + n(t) \right\} * \sum_{m=0}^{N_c-1} c_m^{(1)} p_{rec}(t - mT_c) dt \ . \tag{4.9}$$

Further, n_a can be simplified and expressed as $n_a = n_{am} + n_{ar}$, where n_{am} and n_{ar} are the noise components at branch A due to MAI and receiver noise, respectively. The noise component due to MAI, n_{am}, is defined as

$$n_{am} = \int_0^{Tb} \sum_{k=2}^{N_u} S_{rec}^{(k)}(t) * \sum_{m=0}^{N_c-1} c_m^{(1)} p_{rec}(t - mT_c) dt \ . \tag{4.10}$$

After simplifying Equation (4.10), n_{am} is expressed as

$$n_{am} = \sum_{k=2}^{N_u} d_l^{(k)} \left\{ C_{k,1}^{(0)} \right\} \ , \tag{4.11}$$

where $\left\{ C_{k,1}^{(0)} \right\}$ is the synchronous cross-correlation function between the desired and interfering users during the l^{th} bit interval. Now the expression for n_{ar} is defined as

$$n_{ar} = \int_0^{Tb} n(t) * \sum_{m=0}^{N_c-1} c_m^{(1)} p_{rec}(t - mT_c) dt \ . \tag{4.12}$$

Under the assumption in [42] n_{ar} has Gaussian distribution with zero-mean and variance σ^2_{reca}, where

$$\sigma^2_{reca} = N_c E_p \sigma^2_n = E_b \sigma^2_n \ . \tag{4.13}$$

Therefore, the variable statistic α_a for branch A in its compact form is expressed as

$$\alpha_a = m_a + n_{ar} + n_{am} \ . \tag{4.14}$$

The obtained expression for the variable statistic, α_a, will assist in deriving the final expression for the average probability of error of the proposed receiver.

4.3.2 DS-DPSK Receiver - Branch B

The correlator output in Figure 4.7 is given by

$$\alpha_b = \int_0^{T_b} r(t - T_b) q(t - T_b) dt \ . \tag{4.15}$$

As before, the assumption hereafter is that user 1 currently receiving data, and the l^{th} data bit will be detected. In this case, the despread signal out of the PN code generator module is expressed as

$$q(t - T_b) = \sum_{m=0}^{N_c - 1} c_m^{(1)} p_{rec}(t - (l+1)T_b - mT_c) \ , \tag{4.16}$$

and the received signal after simplification is expressed as

$$r(t - T_b) = \sum_{n=0}^{N_c - 1} d_l^{(1)} c_n^{(1)} p_{rec}(t - (l+1)T_b - nT_c) + n_s \ , \tag{4.17}$$

where $n_s = \sum_{k=2}^{N_u} S_{rec}^{(k)}(t - T_b) + n(t - T_b)$ is the noise source at branch B including MAI and receiver noise $n(t)$, and excluding the signal of the desired user. $S_{rec}^{(k)}(t - T_b)$ is the received signal of k^{th} user at receiver input. Using Equation (4.15), α_b at the l^{th} data bit is defined as

$$\alpha_b = \int_0^{T_b} \left\{ \sum_{n=0}^{N_c-1} d_l^{(1)} c_n^{(1)} p_{rec}(t - T_b - nT_c) + n_s \right\} * \sum_{m=0}^{N_c-1} c_m^{(1)} p_{rec}(t - T_b - mT_c) dt \ . \tag{4.18}$$

Let $\alpha_b = m_b + n_b$, where m_b and n_b are the desired signal and the noise source components at branch B. The desired signal component m_b is defined as

$$m_b = \int_0^{T_b} \sum_{n=0}^{N_c-1} d_l^{(1)} c_n^{(1)} p_{rec}(t - T_b - nT_c) \ * \sum_{m=0}^{N_c-1} c_m^{(1)} p_{rec}(t - T_b - mT_c) dt = N_c E_p d_{l-1}^{(1)} = E_b d_{l-1}^{(1)} \ , \tag{4.19}$$

and the noise component n_b is defined as

$$n_b = \int_0^{Tb} n_s * \sum_{m=0}^{N_c-1} c_m^{(1)} p_{rec}(t - T_b - mT_c) dt \ . \tag{4.20}$$

Therefore n_b can be expressed as

$$n_b = \int_0^{Tb} \left\{ \sum_{k=2}^{N_u} S_{rec}^{(k)}(t - T_b) + n(t - T_b) \right\} * \sum_{m=0}^{N_c-1} c_m^{(1)} p_{rec}(t - T_b - mT_c) dt \ . \tag{4.21}$$

Further, n_b can be simplified and expressed as $n_b = n_{bm} + n_{br}$, where n_{bm} and n_{br} are the noise components at branch B due to MAI and $n(t)$, respectively. The noise component due to MAI, n_{bm}, is defined as

$$n_{bm} = \int_0^{Tb} \sum_{k=2}^{N_u} S_{rec}^{(k)}(t - T_b) * \sum_{m=0}^{N_c-1} c_m^{(1)} p_{rec}(t - T_b - mT_c) dt \ . \tag{4.22}$$

After simplifying Equation (4.22), n_{bm} is expressed as

$$n_{bm} = \sum_{k=2}^{N_u} d_{l-1}^{(k)} \left\{ C_{k,1}^{(0)} \right\} \ , \tag{4.23}$$

where $\left\{ C_{k,1}^{(0)} \right\}$ is the synchronous cross-correlation function between the desired and interfering users during the $(l-1)^{th}$ bit interval. Now the expression for n_{br} is defined as

$$n_{br} = \int_0^{Tb} n(t - T_b) * \sum_{m=0}^{N_c-1} c_m^{(1)} p_{rec}(t - T_b - mT_c) dt \ . \tag{4.24}$$

Similar to n_{ar} in Equation (4.12), n_{br} has Gaussian distribution with zero-mean and variance σ^2_{recb}, where

$$\sigma^2_{recb} = N_c E_p \sigma^2_n = E_b \sigma^2_n \ . \tag{4.25}$$

Therefore, the variable statistic α_b for branch B in its compact form is expressed as

$$\alpha_b = m_b + n_{br} + n_{bm} \ . \tag{4.26}$$

The obtained expression for the variable statistic, α_b, will assist in deriving the final expression for the average probability of error of the proposed receiver.

4.4 DS-DPSK Receiver - Probability of Error Analysis

The randomness of the used PN code sequences with the existence of more than one active-user concurrently in the system permits the approximation of MAI terms, n_{am} and n_{bm}, as Gaussian random processes in Equations (4.14) and (4.26) [43]. Therefore, the variable statistic α_a is expressed as

$$\alpha_a = m_a + n_a, \ \text{where } n_a = n_{ar} + n_{am} \ , \tag{4.27}$$

and the variable statistic α_b is expressed as

$$\alpha_b = m_b + n_b, \ \text{where } n_b = n_{br} + n_{bm} \ . \tag{4.28}$$

Referring to Figure 4.7, the decision statistic Z is equal to the multiplication of the variable statistics α_a and α_b. Assuming that the data bit "1" is transmitted, then the current and previous bits of DPSK signal are the same, hence $m_a = m_b$. Therefore, Z after simplification is expressed as

$$Z = m_a^2 + m_{ab} + n_{ab} \ , \tag{4.29}$$

where $m_{ab} = m_a * [n_a + n_b]$ and $n_{ab} = n_a * n_b$. If the desired signal component m_a in Equation (4.7) is squared, then

$$m_a^2 = (N_c E_p d_l^{(1)})^2 = (E_b d_l^{(1)})^2 = E_b^2 \ . \tag{4.30}$$

Since the receiver noise, $n(t)$, is modeled as an AWGN process with zero-mean (i.e., dc power equal to zero), its variance σ_n^2 (i.e., ac power), is equal to the spectral (i.e., total) power of this process, therefore, σ_n^2 is equal to $N_o/2$. Substituting the value of σ_n^2 in Equation (4.13) , the statistics for n_{ar} are given by $E[n_{ar}] = 0$, and $var[n_{ar}] = E_b\sigma_n^2 = E_b N_o/2$. The statistics for n_{am} are given by $E[n_{am}] = 0$ and $var[n_{am}] = (K-1) * (E_b/N_c)^2$ after approximating MAI term with a Gaussian random process, and considering the effect of other active-users in the system. Therefore, the statistics for the total noise, n_a, at branch A are given by

$$E[n_a] = 0, \text{ and } var[n_a] = E_b N_o/2 + (K-1) * (E_b/N_c)^2 \ . \tag{4.31}$$

Since n_b and n_a have the same statistics, due to the randomness and the independence of the Gaussian processes, and because the sum of two independent random processes is the sum of their statistics, therefore m_{ab} has zero-mean expected value and variance given by

$$var[m_{ab}] = E_b N_o + 2 * (K-1) * (E_b/N_c)^2 \ . \tag{4.32}$$

The statistics for the third term on the right-hand side in Equation (4.29) were derived using Shannon's sampling theorem [16]. The variable n_{ab} can be expressed as

$$n_{ab} = \int_0^{T_b} n_a * n_b dt = \int_0^{T_b} g(t) * g(t+T_b) dt \ , \tag{4.33}$$

where $g(t)$ is a Gaussian random process with zero-mean, and variance $\sigma_g^2 = N_o/2 + 1/N_c^2$. Its autocorrelation function is given by

$$\mathcal{R}(\tau) \stackrel{def}{=\!=} E[g(t) + g(t+\tau)] = (N_o/2 + 1/N_c^2)\delta(t-\tau) \ . \tag{4.34}$$

The sampled version of n_{ab} can be expressed as

$$n_{ab} = \sum_{x=0}^{N} g(x)\delta(t - x/2\beta) \sum_{y=0}^{N} g(y + N)\delta(t - y/2\beta) , \tag{4.35}$$

where $N = 2\beta T_b$ is the number of independent samples per bit, and β is the bandwidth of the 2^{nd} derivative Gaussian pulse. $g(x)$ and $g(y + N)$ are independent and identically distributed (i.i.d) samples from the sampled version of the Gaussian process. Each sample has zero-mean and variance equal to $N_o/(2\sqrt{cl}) + 1/(\sqrt{cl}N_c^2)$ as a result of energy normalization as dictated by the simulation code, where *cl* is the length of the used PN code sequence. Because the bit-period (T_b) is much greater than the sampling-period ($1/2\beta$), using the following approximation

$$\int_0^{T_b} \delta(t - x/2\beta)\delta(t - y/2\beta)dt = \{^{1:x=y}_{0:x\neq y} , \tag{4.36}$$

n_{ab} expression is further simplified and expressed as

$$n_{ab} = \sum_{x=0}^{N} g(x)g(x + N) = \sum_{x=0}^{N} N_x , \tag{4.37}$$

when $y = x$. Therefore, the statistics for N_x are given by $E[N_x] = 0$, and $var[N_x] = var[g(x)] * var[g(x+N)] = [N_o/(2\sqrt{cl}) + 1/(\sqrt{cl}N_c^2)]^2 = 1/cl\ [N_o/2 + 1/N_c^2]^2$. Because each sample has a Gaussian distribution, the sum of the entire N independent samples also has a Gaussian distribution by applying the Central Limit Theorem principle. Therefore n_{ab} has a Gaussian distribution with zero-mean expected value and variance given by

$$Var[n_{ab}] = (K - 1)2\beta T_b/cl * [No/2 + 1/N_c^2]^2 , \tag{4.38}$$

after including the effect of other active-users in the system. The signal-to-noise ratio (γ_b) is given by

$$\gamma_b = \frac{m_a^2}{var[m_{ab}] + var[n_{ab}]} \tag{4.39}$$

Substituting the relevant terms from Equations (4.30), (4.32) and (4.38) in Equation (4.39), the analytical expression for γ_b is given by

$$\gamma_b = \frac{E_b^2}{E_b N_o + 2 * (K-1) * (\frac{E_b}{N_c})^2 + \frac{2\beta T_b}{cl} * [\frac{N_o}{2} + \frac{1}{N_c^2}]^2} \tag{4.40}$$

By substituting the obtained expression, γ_b, in the known expression for the average probability of error of DPSK receiver in AWGN channel, namely $P_e = 0.5 \exp(-\gamma_b)$, the final expression for the average probability of error for the proposed receiver can be obtained analytically.

4.5 Chapter Summary

The focus of this chapter was mainly on introducing the proposed system, its constituent modules, and its associated mathematical representations and analytical derivations. The proposed system consisted of three main modules, namely the transmitter, the channel and the receiver. The transmitter has implemented the noncoherent bit-level DPSK modulation combined with DS-CDMA for multiple-access support. The channel effect under consideration was the AWGN with multiple-access. The unavoidable receiver noise was modeled as an AWGN process. The simultaneous multiple-access for the channel has introduced the multiple-access interference channel effect, which resulted from the cross-correlation among the utilized PN code sequences of the active-users within the system. The multiple-access interference was approximated as an AWGN process. The proposed receiver is the noncoherent bit-level differential-detector that has two branches, namely branch A and branch B, where branch B is the delay-branch that is always delayed by one bit-period. Each of the previously mentioned modules has its own components, which was described mathematically based on its constituent components to come up with a unique mathematical expression that describes the module under consideration. The resulted mathematical expressions are used in later sections in this chapter, and assisted in deriving the analytical expression for the average probability of error of the proposed receiver. The employed analytical method in this work has provided the best approximate solution for the average probability of error of the proposed DS-DPSK receiver. The derived analytical expression depends mainly on the employed system parameters. By examining the derived Signal-to-Noise Ratio (γ_b) expression of the proposed receiver, one can see that the expression was mainly formed using the system parameters those defined within the simulation code of DS-DPSK system.

CHAPTER 5

SIMULATION APPROACH

5.1 Introduction

This chapter covers the accomplished baseband simulation using Matlab for DS-DPSK (proposed) and DS-BPSK (reference) systems, as well as the obtained simulation results, and the calculated statistical measures. This chapter is organized as in the following. Section 5.2 presents the simulation setup for DS-DPSK and DS-BPSK systems.

Section 5.3, provides the obtained simulation results. Three main subsections are included under this section focusing mainly on comparing both systems in terms of bit error rate (BER) performance, as well as defining a new performance metric for verifying the multiple-access (MA) efficiency of DS-DPSK receiver, and comparing the calculated with the measured data to confirm the accuracy of the performed analytical derivations.

Section 5.4, presents some calculated statistical measures on the obtained simulation data of the proposed system, and presents the results in the form of tables. These statistical measures are necessary to confirm the accuracy of the resulted simulation data for the proposed system.

Finally, a brief summary is provided in Section 5.5 aimed to highlight the main points that was covered in this chapter.

5.2 Simulation Setup

The information sources from all active-users in both systems are generated using the built-in Matlab function **randsrc**. They are modeled as random binary bits with non-return-to-zero line coding and transmitted in blocks of 10 information bits. In DS-DPSK system these blocks are initially DPSK modulated. The repetition factor NS for the code repetition coder (CRC) component in the transmitter, which represents a simple forward error correction (FEC) scheme, was set to 1. In this case, the error correction scheme aimed to improve the BER performance is not considered in both systems.

In both systems each information bit is represented by a number of short-duration pulses (square pulses) to follow the idea of IR-UWB radio transmission techniques. A pseudo-noise (PN) code generator used to generate Gold code sequences with lengths equal to the number of pulses per information bit. In this case, the pulses per bit, hence the stream of pulses in the transmitted blocks, are periodically amplitude-modulated based on the constituent code elements of the gold code sequences.

Each pulse in this steam is then mapped to the second derivative of Gaussian pulse that mathematically defined as

$$W_{tx/rec}(t) = [1 - 4\pi(t/\tau_m)^2]\exp[-2\pi(t/\tau_m)^2] \tag{5.1}$$

where $\tau_m = 0.2$ nanosecond (ns), and the pulse width $T_w = 0.5\ ns$. After applying the fractional bandwidth definition of UWB signal, it was found that each pulse of the transmitted stream of the second derivative Gaussian pulses is instantaneous and occupies a broad bandwidth of 6 GHz. Figure 5.1 depicts the time domain representation for the utilized second derivative Gaussian pulse and its power spectral density (PSD) contents in frequency domain.

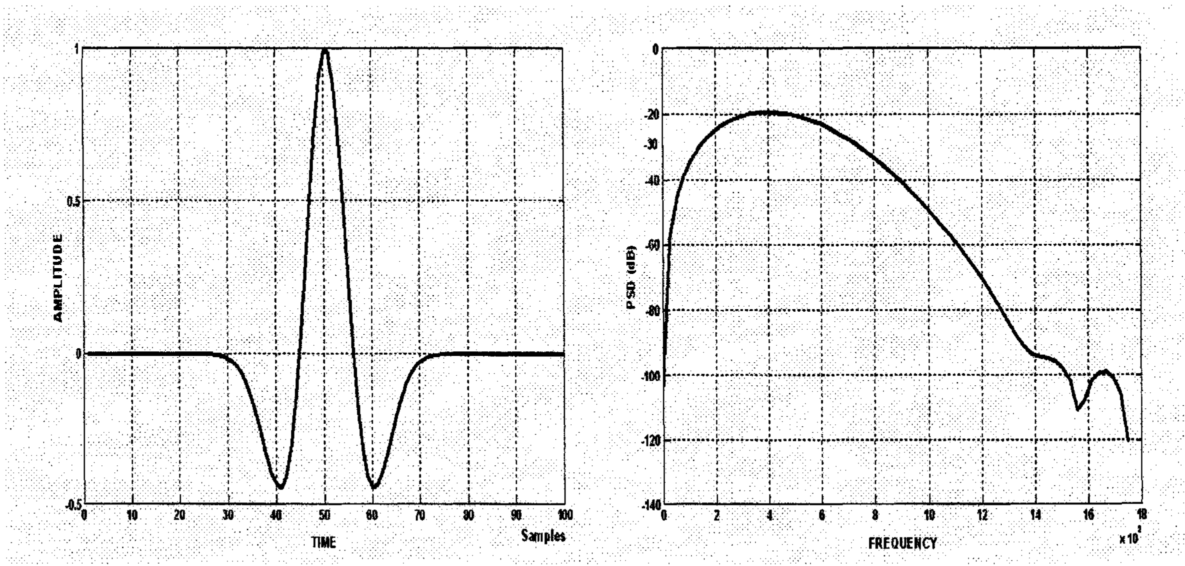

Figure 5.1: 2^{nd} Derivative Gaussian Pulse - Time (left) and PSD (right)

The multiple-access (MA) channel is represented by the sum of all simultaneous signals transmitted by the current active-users within the system under consideration. A custom-made program that uses the built-in Matlab function **randn** is coded to model the unavoidable additive receiver noise. The **randn** function is used to generate random entries, chosen from a normal (Gaussian) distribution with zero-mean and variance equal to 1. The power spectral density of this noise is chosen such that to have value equal to No/2. Since the random noise is coded such that it is always exist, the outcome of the custom-made program is the AWGN random process.

Since the proposed receiver is functioning based on bit-level differential-detection, it is coded such that to have two branches. One of them is the delay branch that uses a bit-period delay component, which provides the template signal that is necessary for demodulation. The decision threshold unit is coded such that it work based on the soft-decision idea for detecting the threshold. The threshold is set equal to zero because the transmitted binary streams of information bits are equally probable.

In the simulation program, the length of the unique gold code sequence cl for each user is equal to the number of pulses per bit N_c. Both are chosen to have value equal to 7, and the pulse repetition period T_c is equal to $1ns$. Therefore, the expected data rate for the proposed system is $R_b = 1/(N_c * T_c) = 1/(cl * T_c) \approx 150$ Mbps per user. In both systems (DS-DPSK and DS-BPSK) the interferers are chosen to be 1, 2 and 3 such that the total number of active-users under study is 4.

5.3 Simulation Results

This section is dedicated mainly to exhibit the obtained results, either the simulated or the calculated using the derived probability of error (P_e) expression, after substituting system parameters and representing the results in the form of graphs. The main idea is to consider these graphs and to compare the obtained results visually. The correct function of the proposed receiver as a noncoherent differential-detector, in addition to its multiple-access (MA) efficiency is verified. The accuracy of the derived P_e expression is either confirmed in this section.

5.3.1 BER performance Comparisons - DS-DPSK and DS-BPSK

The comparison between the proposed noncoherent DS-DPSK receiver and the reference coherent DS-BPSK receiver, in terms of bit error rate (BER) performance is the main concern in this subsection. Because the BER performance of the reference receiver is known to be optimal, and the BER performance loss as a result of using noncoherent receivers is expected to fall within 3 dBs range, if the BER performance loss of the proposed noncoherent receiver is within the expected range, then it will be considered as a functional noncoherent receiver. Performance comparison between both receivers for the required signal to noise ratio (SNR) level in dB, which is necessary to achieve BER=10^{-3} for different number of active users is shown in Figure 5.2.

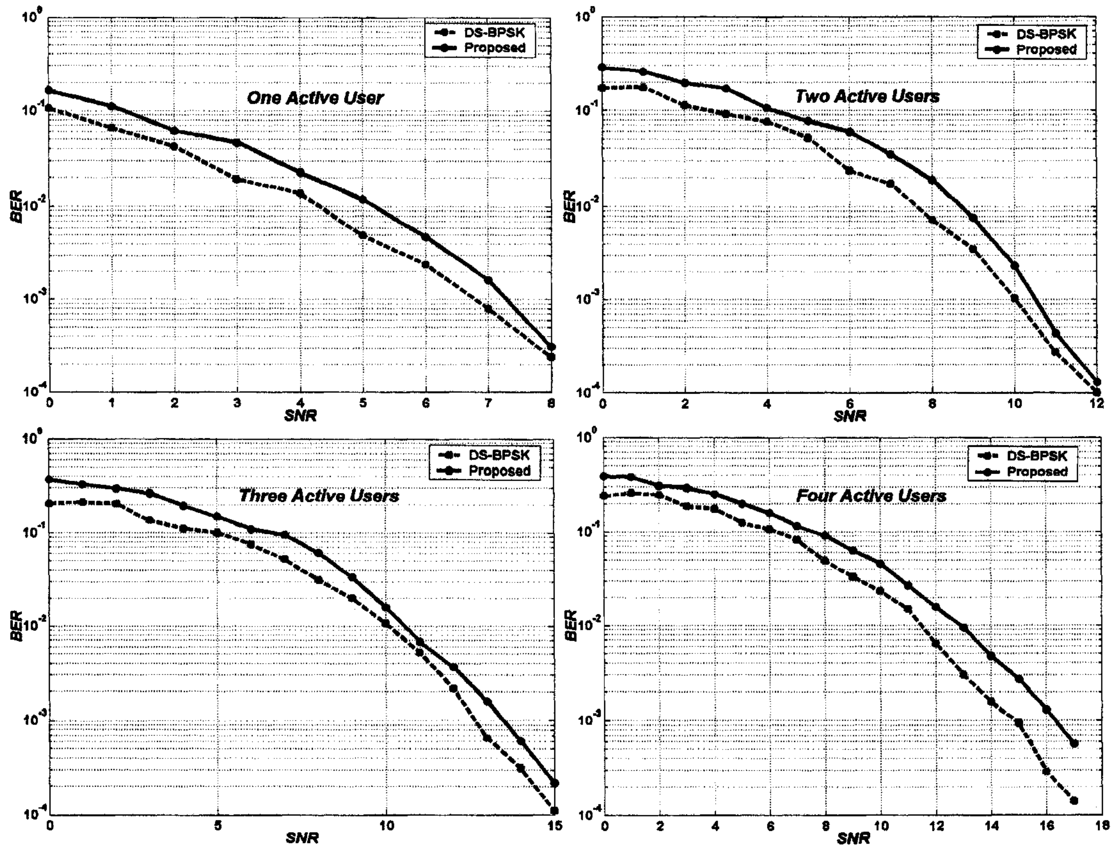

Figure 5.2: BER *vs* SNR Comparisons (DS-BPSK and DS-DPSK Receivers)

Because any communications receiver that is capable of producing BER performance level equal to 10^{-3} is considered a functional receiver, the required SNR levels in both systems necessary to achieve this performance level are chosen to reflect the performance of both receivers. For different scenarios of having different number of active-users these SNR levels are extracted from Figure 5.2 and tabulated in Table 5.1.

Table 5.1: SNR levels in dB necessary to achieve BER = 10E-3 in both receivers

	One-Active	**Two-Active**	**Three-Active**	**Four-Active**
DS-BPSK (a)	6.8	10	12.6	15
DS-DPSK	7.2	10.6	13.7	16.2
Difference (b)	0.4	0.6	1.1	1.2
PD $=\frac{(b)}{(a)}$***100** (%)	5.8	6	8.7	8

Referring to Table 5.1, when both receivers have the full capacity of four active-users, it is shown that the maximum increase in the required SNR level necessary to achieve BER=10^{-3} in DS-DPSK receiver relative to DS-BPSK receiver is 1.2 dB. Since the maximum increase is within the 3 dBs range, the proposed receiver can be considered as a functional noncoherent IR-UWB receiver, which is functioning based on the bit-level differential-detection scheme.

As shown in Figure 5.2, the slight BER performance improvement of the proposed receiver is the result of using the pseudo-noise (PN) code sequences in conjunction with DPSK modulation. The PN code sequences (i.e., the gold codes) are responsible for supporting and improving the multiple-access capability of DS-DPSK system. In addition, they are responsible for smoothing the spectrum of the transmitted DS-DPSK signal by reducing the interfering effects of its spectral lines. Therefore, the gold codes are responsible for reducing the co-channel interference effects, as well as the interference effects on other radio systems. Hence, they are responsible for improving the overall BER performance of DS-DPSK receiver.

5.3.2 Multiple-Access Efficiency - DS-DPSK Receiver

The behavior of the simulation graphs as shown in Figure 5.3 has motivated the definition of a new performance metric, which is called by the multiple-access efficiency (MAE) metric, and is intended to test the MA efficiency of DS-DPSK receiver in handling the increase in the number of active-users in DS-DPSK system.

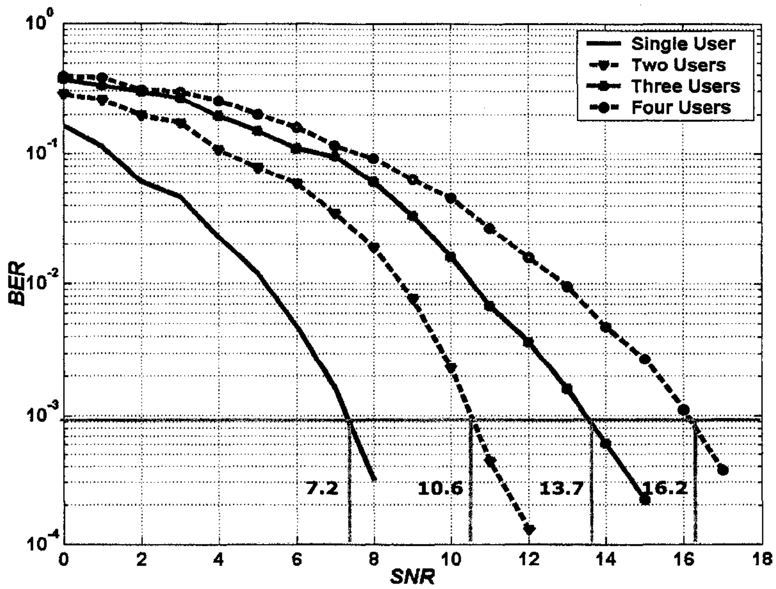

Figure 5.3: BER *vs* SNR Comparisons (DS-DPSK Receiver)

As shown in Figure 5.3, one can see the convergence in the distance between every subsequent graph, where the convergence is more between the graphs representing the higher number of active-users cases in the proposed DS-DPSK system. The multiple-access efficiency (MAE) metric is nothing more than the mathematical expression that represents the inverse of this convergence in percentage, which in turn, reflects the increase in the required SNR levels as a result of increasing the number of active-users in the proposed DS-DPSK system. Since this metric is basically based on a simple mathematical relationship, it is expected to perform its required task. The MAE metric mathematically defined as

$$MAE = [10^{(SNR_{cc}-SNR_{pc})/10}]^{-1} * 100 \tag{5.2}$$

where SNR_{cc} and SNR_{pc} are defined as in the following. At BER performance level equal to 10^{-3}, if the number of active-users in DS-DPSK system has increased from the single active-user case to the two active-users case, then, SNR_{pc} value is equal to 7.2 dB and SNR_{cc} value is equal to 10.6 dB as shown in Figure 5.3. These values are resulted from projecting the intersection points, between the horizontal line at BER=10^{-3} with the shown graphs, on the horizontal SNR axis. Following the same procedure, while the number of active-users is increasing from the two active-users case to the three active-users case, and from the three active-users case to the four active-users case, respectively, the calculated values out of the MAE metric are given by:

$$MAE = [10^{(10.6-7.2)/10}]^{-1} * 100 = 45.63 \ \%$$

$$MAE = [10^{(13.7-10.6)/10}]^{-1} * 100 = 49.1 \ \%$$

$$MAE = [10^{(16.2-13.7)/10}]^{-1} * 100 = 56.6 \ \%$$

The calculated results out of MAE performance metric reflected that the required increase in SNR level, which is necessary to achieve BER equal to 10^{-3}, is getting smaller as the number of active-users in DS-DPSK system is getting higher. Therefore, the required increase in SNR is bounded for the case when DS-DPSK system has the full capacity of active-users. Hence, DS-DPSK receiver is capable of handling the increase in the number of active-users efficiently. The MAE performance metric can be used to define the upper bound for the required increase in SNR levels, especially, when it approaches 100% value as a result of the continuous increase in the number of active-users in DS-DPSK system. In that case, the previous and the current graphs will coincide with each other. Therefore, any further increase in SNR level (i.e., beyond the upper bound) has no effect in improving the BER performance. Hence, the maximum theoretical number of active-users those can coexist concurrently at the input of DS-DPSK receiver, while the user of interest is receiving its information bits, is also approached. MAE performance metric has confirmed the applicability of the proposed receiver as an efficient noncoherent IR-UWB receiver for multiple-access support.

5.3.3 DS-DPSK BER Comparisons - Analyses and Simulations

A comparison between the analyzed and the simulated bit error rate (BER) for different number of active-users in DS-DPSK system is shown in Figure 5.4.

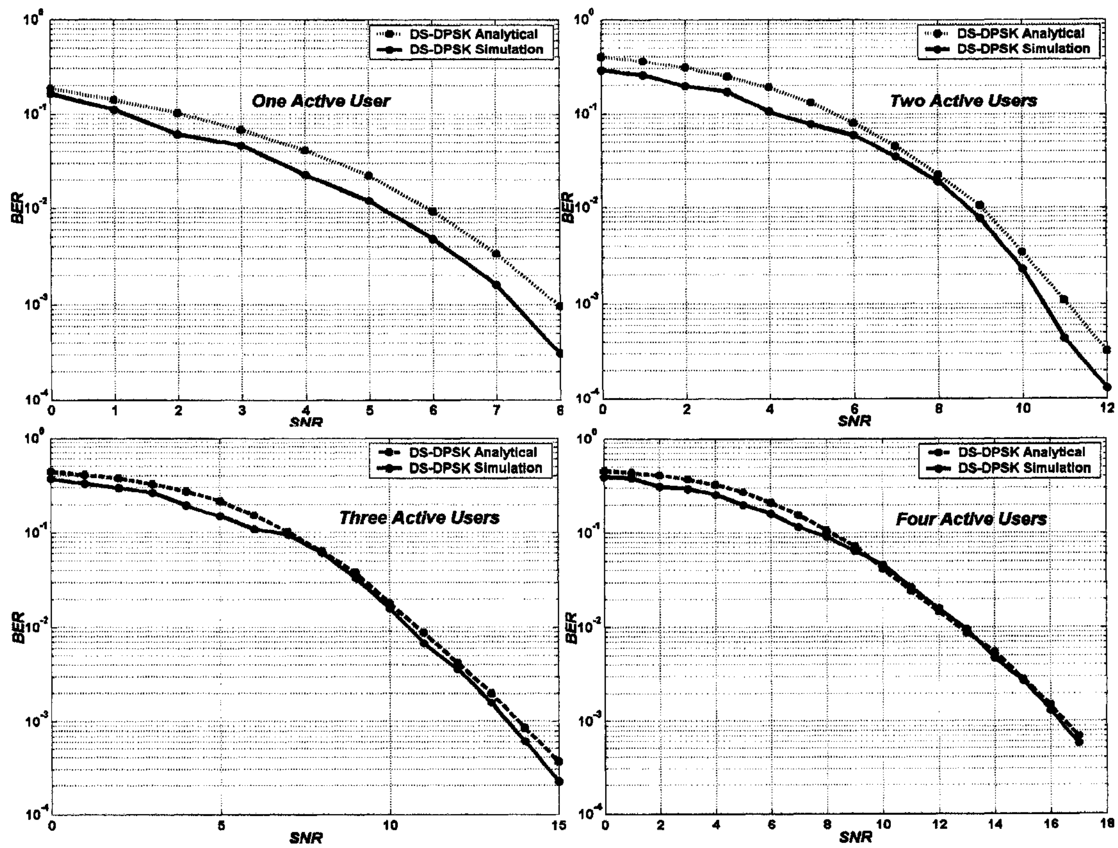

Figure 5.4: BER *vs* SNR (Analytical and Simulation) DS-DPSK Receiver

The purpose of the performed comparisons shown in Figure 5.4 is to confirm the accuracy of the derived average probability of error expression of DS-DPSK receiver. In that figure, simulation graphs behaved as the lower-limit for the incurred BER in DS-DPSK receiver while analytical graphs behaved as the upper-limit. For each case of having different number of active-users in DS-DPSK system, both graphs (i.e., analytical and simulation) are close enough and change in accordance to each other.

As mentioned previously in this thesis, the multiple-access interference which is resulted from the simultaneous channel accessing by many active-users in DS-DPSK system, is approximated as a Gaussian random process. This approximation becomes more valid as the number of active-users is increased as a result of applying the Gaussianity principle of the central limit theorem. Therefore, as shown in Figure 5.4, when the number of active-users in DS-DPSK system is increased, both graphs turn out to be closer to each other.

The conducted comparisons are sufficient evidence on the correctness of the performed mathematical representations, and analytical derivations for the average probability of error of DS-DPSK receiver.

5.4 Statistical Measures - DS-DPSK System

To describe the behavior and provide the best estimate for the resulted simulation data of DS-DPSK system, statistical measures such as the mean, the standard deviation, the average deviation, and the average relative error are calculated and investigated. For different cases of having different number of active-users in DS-DPSK system, each case (or experiment) was repeated five times to get the corresponding dataset, which consists of the resulted BER values at different SNR levels during simulations.

The first measure is the mean (MEAN) value, also known as the arithmetic mean, provides the best estimated means for the BER entries of the dataset for the specific case (or experiment) under consideration.

The second measure is the standard deviation (STD DEV), also known as the absolute error, determines how widely the BER entries of the dataset are dispersed around their estimated means.

The third measure is the average deviation (AVG DEV), also known as the average error, provides the average of the absolute errors. In addition, it measures the variability among the resulted BER entries of the dataset for the specific case (or experiment) under consideration.

The last measure is the average relative error (AVG REL ERR), which is nothing more than dividing the average deviations by their corresponding estimated means to represent these deviations as percentages, in terms of their estimated means.

All the aforementioned statistical measures are calculated for different cases of having different number of active-users in the proposed DS-DPSK system. The results were tabulated in the following four tables. Table 5.2 tabulates the calculated statistical measures for the single active-user case in DS-DPSK system.

Table 5.2: Statistical measures for single active-user case in DS-DPSK system

SNR	MEAN	STD DEV	AVG DEV	AVG REL ERR(%)
0	0.16413	0.00826	0.00770	4.6
1	0.11185	0.01456	0.01364	12.1
2	0.06104	0.00901	0.00862	14.1
3	0.04660	0.00520	0.00504	10.9
4	0.02252	0.00144	0.00132	5.8
5	0.01189	0.00057	0.00049	4.1
6	0.00479	0.00030	0.00027	5.6
7	0.00161	0.00008	0.00008	4.9
8	0.00031	0.00003	0.00003	9.6

Table 5.3 tabulates the calculated statistical measures for the two active-users case in DS-DPSK system.

Table 5.3: Statistical measures for two active-users case in DS-DPSK system

SNR	MEAN	STD DEV	AVG DEV	AVG REL ERR(%)
0	0.28491	0.00700	0.00650	2.2
1	0.25667	0.00295	0.00260	1.1
2	0.19610	0.01025	0.00876	4.4
3	0.17159	0.01477	0.01358	7.9
4	0.10588	0.00156	0.00131	1.2
5	0.07716	0.01054	0.00940	12.1
6	0.05945	0.00581	0.00443	7.4
7	0.03478	0.00268	0.00222	6.3
8	0.01886	0.00156	0.00148	7.8
9	0.00766	0.00091	0.00074	9.6
10	0.00231	0.00019	0.00018	7.7
11	0.00044	0.00005	0.00005	11.3
12	0.00013	0.00003	0.00002	15.3

Table 5.4 tabulates the calculated statistical measures for the three active-users case in DS-DPSK system.

Table 5.4: Statistical measures for three active-users case in DS-DPSK system

SNR	MEAN	STD DEV	AVG DEV	AVG REL ERR(%)
0	0.37073	0.01053	0.01017	2.7
1	0.33043	0.00798	0.00712	2.1
2	0.29608	0.01081	0.00856	2.8
3	0.26552	0.03797	0.03628	13.6
4	0.19359	0.00721	0.00674	3.4
5	0.14902	0.01409	0.01062	7.1
6	0.10935	0.01152	0.00792	7.2
7	0.09438	0.00939	0.00783	8.2
8	0.06103	0.01245	0.01074	17.5
9	0.03335	0.00280	0.00221	6.5
19	0.01597	0.00331	0.00254	15.8
11	0.00681	0.00084	0.00072	10.5
12	0.00363	0.00047	0.00040	10.7
13	0.00159	0.00029	0.00023	13.8
14	0.00061	0.00007	0.00006	9.8
15	0.00022	0.00003	0.00003	13.6

Table 5.5 tabulates the calculated statistical measures for the four active-users case in DS-DPSK system.

Table 5.5: Statistical measures for four active-users case in DS-DPSK system

SNR	MEAN	STD DEV	AVG DEV	AVG REL ERR(%)
0	0.39073	0.00281	0.00257	0.7
1	0.38043	0.03021	0.02904	7.6
2	0.30908	0.01110	0.00954	3.1
3	0.29552	0.01544	0.01139	3.8
4	0.25359	0.03100	0.03003	11.8
5	0.19902	0.00986	0.00847	4.2
6	0.15935	0.01471	0.01117	7
7	0.11438	0.00472	0.00441	3.9
8	0.09103	0.00424	0.00348	3.8
9	0.06335	0.00875	0.00709	11.1
10	0.04597	0.00668	0.00607	13.2
11	0.02681	0.00241	0.00215	8
12	0.01563	0.00126	0.00120	7.6
13	0.00952	0.00110	0.00091	9.5
14	0.00472	0.00033	0.00027	5.7
15	0.00272	0.00043	0.00041	15.1
16	0.00131	0.00018	0.00013	9.9
17	0.00057	0.00003	0.00003	5.2

By considering the above shown four tables, it is shown that the tabulated standard deviations are relatively small, therefore, the resulted BER entries of the dataset are relatively close to each other, and hence the absolute errors are not that significant around their estimated mean.

In addition, the tabulated average deviations are even less than their corresponding standard deviations. Therefore, on average the absolute errors are even less than their tabulated values in the above tables. Average deviations also confirmed that the variability among the resulted BER entries of the dataset, for each considered case (or experiment), is not that significant.

The tabulated average relative errors indicated that the average deviations are small relative to their estimated means, which means that the average errors are small. In general, the above statistical measures have confirmed the accuracy of the obtained simulation data of DS-DPSK system.

5.5 Chapter Summary

In this chapter, the calculated and the simulated data for DS-DPSK and DS-BPSK systems were presented by means of graphs and tables. The underlying algorithm for the simulation code for both systems was based on Monte Carlo simulation method. This simulation method is characterized by the wide existence of random and pseudo-random number generators. Therefore, random errors were expected to occur in addition to the unavoidable system errors. Two important facts concerning the functional aspects of the proposed receiver were confirmed in this chapter. The first is the function of the proposed receiver as a practical noncoherent differential-detector. The second is the capability of this receiver to support multiple-access environments efficiently. The mathematical representations and the analytical derivations for the average probability of error of the proposed receiver were verified via simulations. The observed match between the calculated and the simulated graphs of DS-DPSK system confirmed the accuracy of the derived analytical probability of error expression. As a result of the unavoidable system and random errors, the obtained simulation results for the proposed DS-DPSK system were verified statistically. Statistical measures such as the mean, standard deviation, average deviation, and average relative error were calculated and tabulated. In general, the mean provided the best estimated means for the obtained BER entries of the dataset. The other statistical measures provided mainly to give an idea about the variation around these estimated means. The results of these statistical measures have indicated that the variations are low around the estimated means and they are not that significant. Therefore, the calculated statistical measures were a strong evidence for the well-behavior of the obtained simulation results, and on the accuracy of the performed simulations for the proposed DS-DPSK system.

CHAPTER 6

CONCLUSION

The carrier recovery circuit and channel estimation are required for improving BER performance of coherent IR-UWB receivers. Both requirements increase design complexity and power consumption of coherent IR-UWB receivers. Noncoherent IR-UWB receivers, such as the noncoherent differential-detectors, are often proposed to bypass the carrier recovery circuit and channel estimation requirements. Therefore, noncoherent IR-UWB receivers are simple in their design, but their BER performance is inferior relative to the performance of coherent IR-UWB receivers.

In this thesis, a novel noncoherent (i.e. differential-detector) receiver was proposed for Impulse-Radio Ultra-Wideband (IR-UWB) communication systems that support multiple-access. The transmitter of the proposed system has employed the noncoherent bit-level differential phase-shift keying (DPSK) modulation combined with direct-sequence code division multiple-access (DS-CDMA). The proposed system has been studied under the additive white Gaussian noise (AWGN) with multiple-access channel effect. The proposed receiver has employed the noncoherent bit-level differential-detection scheme to recover the originally transmitted information bits. As a result of using DS-CDMA combined with DPSK modulation, the entire system was referred to as DS-DPSK system. DS-DPSK receiver was compared against another existing coherent receiver (DS-BPSK) in terms of BER performance to confirm its practicality.

In this thesis, the obtained simulation results indicated that the proposed DS-DPSK (noncoherent) receiver has a slight BER performance loss compared to the reference DS-BPSK (coherent) receiver. The maximum increase in the required SNR level, which is necessary to achieve BER equal to 10^{-3}, as a result of using DS-DPSK receiver was reported about 1.2 dB. Simulation results also confirmed the capability of the proposed DS-DPSK receiver in supporting multiple-access environments efficiently, and the accuracy of the performed analytical derivations for its average probability of error expression. Despite the slight BER performance loss of DS-DPSK receiver, its simple design, as well as its ability to avoid carrier recovery circuit and channel estimation, the proposed DS-DPSK receiver can be successfully used in IR-UWB communication systems.

In this thesis, the proposed DS-DPSK receiver has been studied to test the effect of the free-space (i.e., AWGN) channel, which accounts for multiple-access interference that resulted from the simultaneous channel accessing by many active-users, on its BER performance. As a future consideration, the proposed receiver can be studied to test the effect of multi-path channel on its BER performance, and its capability to capture the transmitted energy from the scattered multi-path components. Another issue to consider is to determine the maximum number of active-users those can coexist simultaneously, while the user of interest is receiving its information bits, and without affecting the BER performance of the proposed DS-DPSK receiver adversely.

BIBLIOGRAPHY

[1] FCC notice of proposed rule making, revision of part 15 of the commission's rules regarding ultra-wideband transmission systems,"Federal Communications Commission, Washington, DC, ET-Docket 98-153, 2002".

[2] S. Roy, J. Foerster, V. Somayazulu and D. Leeper,"Ultrawideband radio design: the promise of high-speed, short-range wireless connectivity," IEEE communications journal, vol. 92, issue 2, pp. 295-311, Feb. 2004.

[3] "SG3a Alternate PHY Selection Criteria," IEEE P802.15-02/105r25 [online]. Available: http://grouper.ieee.org/groups/802/15/pub/2002/Sep02/, 2002.

[4] D. Wentzloff, R. Blazquez, F. Lee, B. Ginsburg, J. Powell and A. Chandrakasan, "System design considerations for ultra-wideband communication," IEEE Communications journal, vol. 43, issue 8, pp. 114-121, Aug. 2005.

[5] P. Runkle, J. McCorkle, T. Miller and M. Welborn, "DS-CDMA: the modulation technology of choice for UWB communications," IEEE Conference on Ultra Wideband Systems and Technologies., pp. 364-368, 16-19 Nov. 2003.

[6] C. Woo, N. August and S. Dong, "Signaling and multiple access techniques for ultra wideband 4G wireless communication systems," IEEE Wireless Communications journal, vol. 12, issue 2, pp. 46-55, Apr. 2005.

[7] G. Durisi and S. Benedetto, "Comparison between Coherent and Noncoherent Receivers for UWB Communications," EURASIP Journal on Applied Signal Processing, pp. 359–368, Mar. 2005.

[8] G. Durisi and S. Benedetto, "Performance of coherent and noncoherent receivers for UWB communications," IEEE Intl. Conf. on Commun., vol. 6, pp. 3429-3433, 20-24 Jun. 2004.

[9] J. G. Proakis and M. Salehi, Communication Systems Engineering. 2nd edition, Prentice Hall, New Jersey, 2002.

[10] F. Salem, R. Pyndiah and A. Bouallegue, "New multiple access frame differential DS-UWB system," IEEE International conference on Broadband Networks, vol. 2, pp. 1163-1167, Oct. 2005.

[11] L. Piazzo and F. Ameli, "Performance analysis for impulse radio and direct-sequence impulse radio in narrowband interference," IEEE Transactions on Communications, vol. 53, Issue 9, pp. 1571-1580, Sept. 2005.

[12] B. Sadler and A. Swami, "On the performance of episodic UWB and direct-sequence communication systems," IEEE Transactions on Wireless Communications, vol. 3, Issue 6, pp. 2246-2255, Nov. 2004.

[13] M. Win and R. Scholtz, "Impulse radio: how it works," IEEE Communications Letters, vol. 2, pp. 36-38, Feb. 1998.

[14] N. Boubaker and K. Letaief, "Ultra Wideband DSSS for Multiple Access Communications Using Antipodal Signaling," IEEE Intl. Conf. on Commun., vol. 3, pp. 2197-2201, May 2003.

[15] Z. Bai and K. Kwak, “Analysis of multiuser DS-PAM and TH-PPM UWB systems in data and image transmission,” in Proc. IEEE Intl. Conf. on Wireless Commun., Net. and Mobile Comput., vol. 1, pp. 324-327, 23-26 Sep. 2005.

[16] I. Falujah and V. Prabhu, "Performance analysis of PSK systems in the presence of slow fading, imperfect carrier phase recovery, and AWGN," IEE Communications journal, vol. 152, issue 6, pp. 903-911, 9 Dec. 2005.

[17] H. Rohling and T. May, "Comparison of PSK and DPSK modulation in a coded OFDM system," IEEE 47th Conf. on Vehicular Technology, vol. 2, pp. 870-874, May 1997.

[18] P. Marco and J. Gerard, “Analysis and Comparison of Autocorrelation Receivers for IR-UWB Signals Based on Differential Detection,” IEEE Intl. Conf. on Acoustics, Speech, and Signal Proc., vol. 4, pp.513–516, May 2004.

[19] M. Ho, V. Somayazulu, J. Foerster and S. Roy, “A differential detector for an ultra-wideband communications system,” in Proc. IEEE 55th Vehic. Tech. Conf., vol. 4, pp. 1896–1900, Burmingham, Alabama, USA, Spring 2002.

[20] Multispectral Solutions, Inc. - History of UWB Technology, "A Brief History of UWB Communications," [online]. Available: http://www.multispectral.com/history.html.

[21] F. Nekoogar, Ultra Wideband Communications: Fundamentals and Applications. Prentice Hall, New Jersey, 2006.

[22] D. Geer, “UWB standardization effort ends in controversy,” Computer, vol. 39, Issue 7, pp. 13-16, July 2006.

[23] MBOA, "MultiBand OFDM Physical Layer Proposal for IEEE 802.15.3a," IEEE P802.15 Working Group for WPANs, Sept. 2004.

[24] "IEEE 802.15.3a Updated DS-UWB Proposal Specification," IEEE P802.15 Working Group for WPANs, July 2004.

[25] E. Thomas, "UWB regulation in the USA," IEE Seminar on Ultra Wideband Communications Technologies and System Design, pp. 1–16, 8 July 2004.

[26] V. Somayazulu, J. Foerster and S. Roy, "Design challenges for very high data rate UWB systems," Conference on Signals, Systems and Computers, vol. 1, pp. 717-721, 3-6 Nov. 2002.

[27] W. Lee, "Overview of cellular CDMA," IEEE Transactions on Vehicular Technology, vol. 40, Issue 2, pp. 291–302, May 1991.

[28] M. Pursley, "Performance Evaluation for Phase-Coded Spread Spectrum Multiple-Access Communication-Part I: System Analysis," IEEE Transactions on Communications, vol. 25, Issue 8, pp. 795–799, Aug. 1977.

[29] H. Harada and R. Prasad, Simulation and Software Radio for Mobile Communications. Artech House, Boston, 2002.

[30] R. Kohno, R. Meidan and L. Milstein," Spread spectrum access methods for wireless communications," IEEE Communications Magazine, vol. 33, Issue 1, pp. 58–67, Jan. 1995.

[31] J. H. Reed, An Introduction to Ultra Wideband Communications systems. Prentice

Hall, New Jersey, 2005.

[32] Qinghua Li and L. Rusch, "Multiuser detection for DS-CDMA UWB in the home environment," IEEE Journal on Selected Areas in Communications, vol. 20, Issue 9, pp. 1701-1711, Dec. 2002.

[33] K. Seok and L. Byeong, "A theory on sequence spaces and shift register generators," IEEE Transactions on Communications, vol. 44, Issue 5, pp. 609–618, May 1996.

[34] B. Sklar, Digital Communications: Fundamentals and Applications. 2nd edition, Prentice Hall, New Jersey, 2001.

[35] D. H. Morais, Fixed Broadband Wireless Communications: Principles and Practical Applications. Prentice Hall, New Jersey, 2004.

[36] S. Oshita and K. Feher, "Performance of Coherent PSK and DSPK Systems in an Impulsive and Gaussian Noise Environment," IEEE Transactions on Communications, vol. 30, Issue 12, pp. 2540–2546, Dec. 1982.

[37] L. M. Davis and I. B. Collings, "DPSK versus pilot-aided PSK MAP equalization for fast-fadingchannels," IEEE Transactions on Communications, vol. 49, Issue 2, pp. 226-228, Feb. 2001.

[38] G. Bottomley, T. Ottosson and Y. Wang, "A generalized RAKE receiver for DS-CDMA systems," Vehicular Technology Conference Proceedings, 2000, vol. 2, pp. 941–945, 15-18 May 2000.

[39] B. Kim, J. Bae, I. Song, S. Kim and H. Kwon, "A Comparative Analysis of Optimum

and Suboptimum Rake Receivers in Impulsive UWB Environment," IEEE Transactions on Vehicular Technology, vol. 55, Issue 6, pp. 1797–1804, Nov. 2006.

[40] A. Idriss, R. Moorfeld, S. Zeisberg and A. Finger, "Performance of coherent and non-coherent receivers of UWB communication," Second IFIP Intl. Conf. on Wireless and Optical Communication Networks, pp. 117-122, 6-8 Mar. 2005.

[41] Y. Ma, T. Lim and S. Pasupathy, "Error probability for coherent and differential PSK over arbitrary Rician fading channels with multiple cochannel interferers," IEEE Transactions on Communications, vol. 50, Issue 3, pp. 429-441, Mar. 2002.

[42] A. Scholtz, "Multiple access with time-hopping impulse modulation," in Proc. IEEE Conference on Military Communications, pp. 11–14, 1993.

[43] S. Verdu, Multiuser Detection. Cambridge University Press, New York, 1998.

VITA AUCTORIS

Walid M. Mahmoud received his B.A.Sc. Degree in Computer Engineering from the University of Western Ontario, in London, Ontario, Canada in 2004. In 2005, he came to the Department of Electrical and Computer Engineering at the University of Windsor, in Windsor, Ontario, Canada for his M.A.Sc. Degree in Electrical Engineering, with concentration in the communication area. His Master of Applied Science research focused on wireless communication receivers design for Ultra-Wideband (UWB) technology. He was rewarded the In-Program Scholarship during the course of his M.A.Sc. Degree. His research interests include wired and wireless communications systems, signal processing for communications, computer networks and computer security. He is a student member of the IEEE.